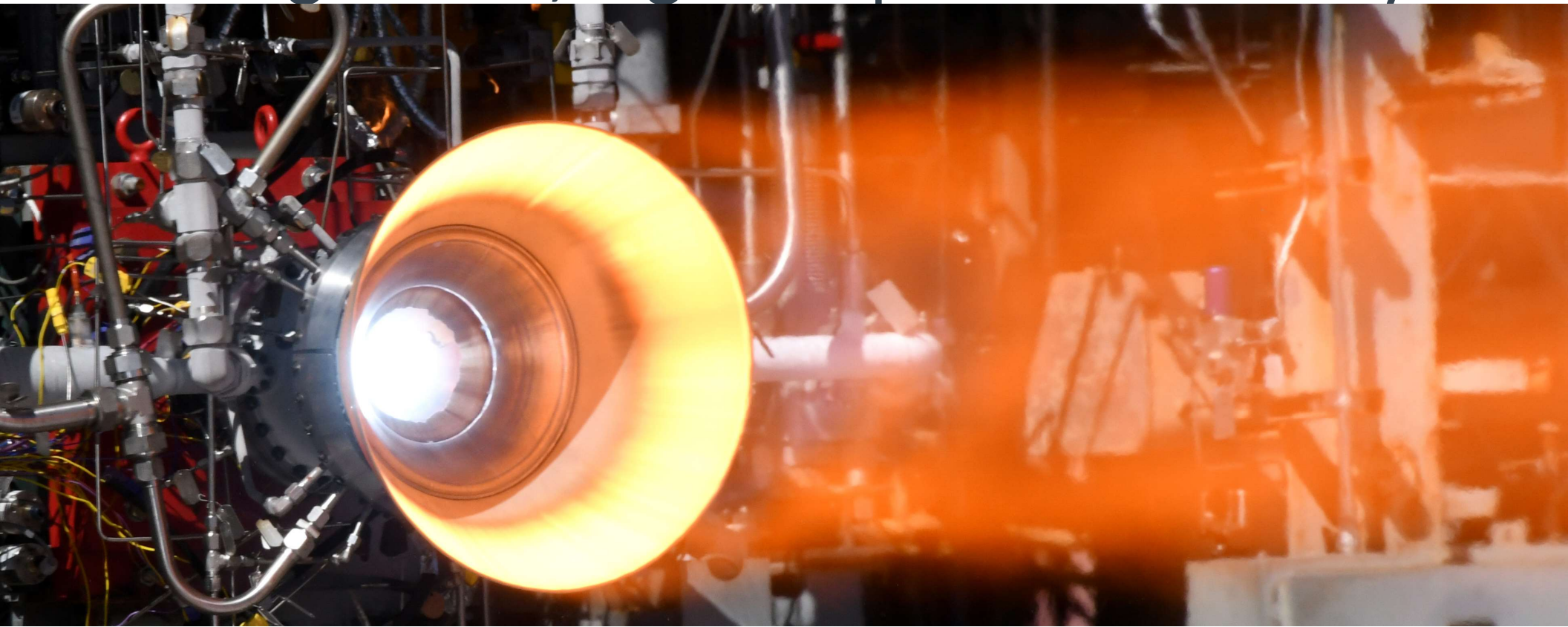


Expansion of additive manufacturing capabilities into in situ alloying of dispersion strengthened, high temperature Cu alloys



David Scannapieco¹, David L. Ellis², and John Lewandowski¹

¹*Case Western Reserve University, Cleveland, OH*

²*Glenn Research Center, Cleveland, OH*

Acknowledgements

Support is provided by NASA Grant NASA-80NSSC19K1736 ‘In-situ alloying of GRCop-42’, NASA ULI: NASA-80NSSC19M0123 ‘Development of an Ecosystem for Qualification of AM Processes and Materials in Aviation’, and CWRU’s Arthur P. Armstrong Professorship.

Additionally, this work would not be possible without our excellent colleagues at:

NASA GRC

Dereck Johnson
Aaron Thompson
Wayne Jennings
Joy Buehler
Laura Evans
Pete Bonacuse
Cheryl Bowman
Richard Rogers
Gustavo Costa

NASA MSFC

Paul Gradl
Chris Protz
John Fikes
Parker Shane
Tim Poe

CWRU

Jackson Smith
Jennifer Carter
Rich Tomazin

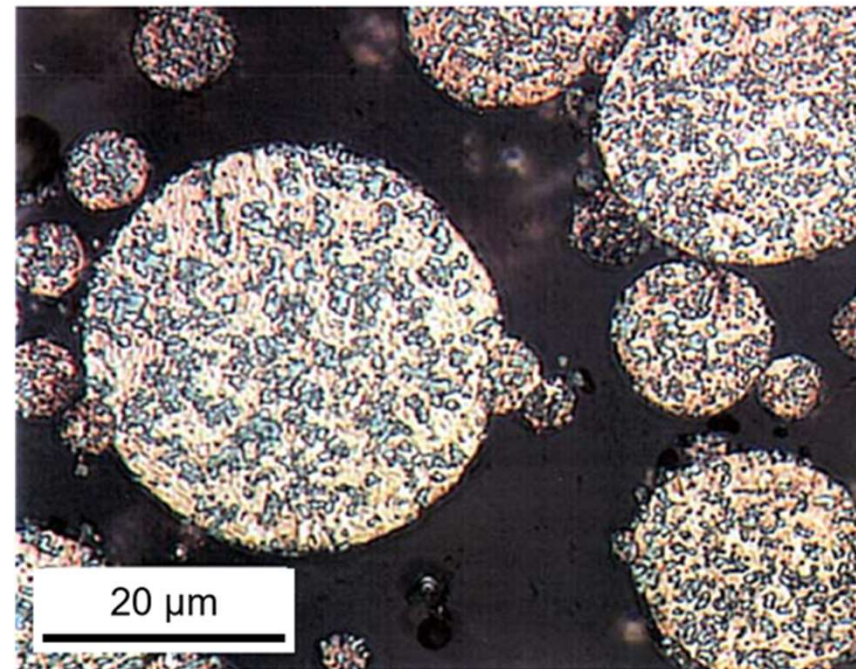
CMU Led NASA ULI

Overview

- Background
- Single Track experiments
- Weld Pool Model
- Powder manufacturing
- In situ alloying analysis
 - Powder influence
 - Laser Power Influence
 - Laser Velocity Influence
- Dispersoid chemistry and morphology comparison
- Conclusions

Background: GRCop

- Family of Cu-Cr-Nb alloys with pure Cu matrix with Cr_2Nb dispersoid
 - GRCop-42: Cu-4 at% Cr-2 at% Nb
 - Conventionally processed by gas atomization.
- Designed for:
 - High temperature mechanical properties
 - High thermal conductivity¹
- Additive manufacturing (AM) provides increased design freedom and advanced alloying capabilities
- Challenges:
 - Reaction for Cr_2Nb occurs at Cu melting temperatures
 - High reflectivity of Cu makes most lasers a challenge to work with.
 - Green laser or e-beam is preferred, but not always available.

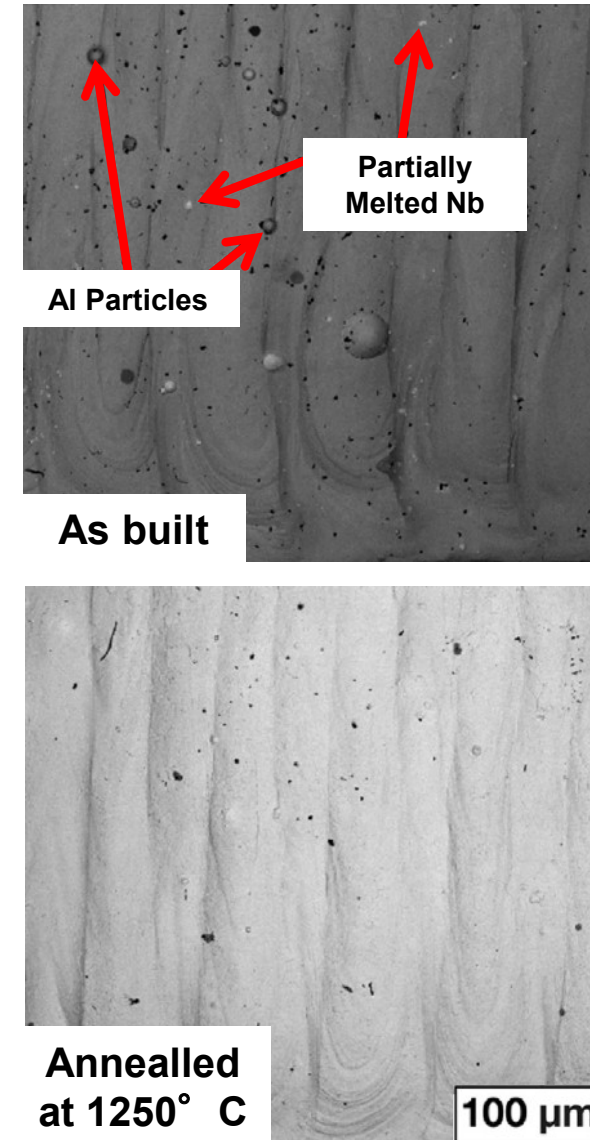


³D. L. Ellis, NASA TM - 2005-213566, 2005.

²K. G. Cooper, et al. NASA TM -2018-220129, 2018.

Background: In Situ Alloying via AM

- Current Literature:
 - Binary or ternary intermetallic alloys.
 - All elements participate in the reaction (Ti-Al, Ti-Al-Nb, Ti-B, etc.)
 - Post-processing can be used to “fix” microstructural issues, shown right.
- Our work:
 - Dispersion-strengthened alloy
 - Cu does not participate in the alloying process
 - Reacting Cr_2Nb in melt pool
 - Heat treatment cannot necessarily be used to “fix” microstructure
 - Nb has little diffusivity in solid Cu



Background: In Situ Alloying via AM

- Literature suggests in situ alloying needs higher wattage at the same energy per volume in order to produce fully dense components.
 - This seems contradictory because:
 - In situ alloying, in this case, contains an exothermic reaction.
 - Prior milling potentially produces intermediary phases which react more readily.
- **Can this energy discrepancy be addressed with an analytical model?**

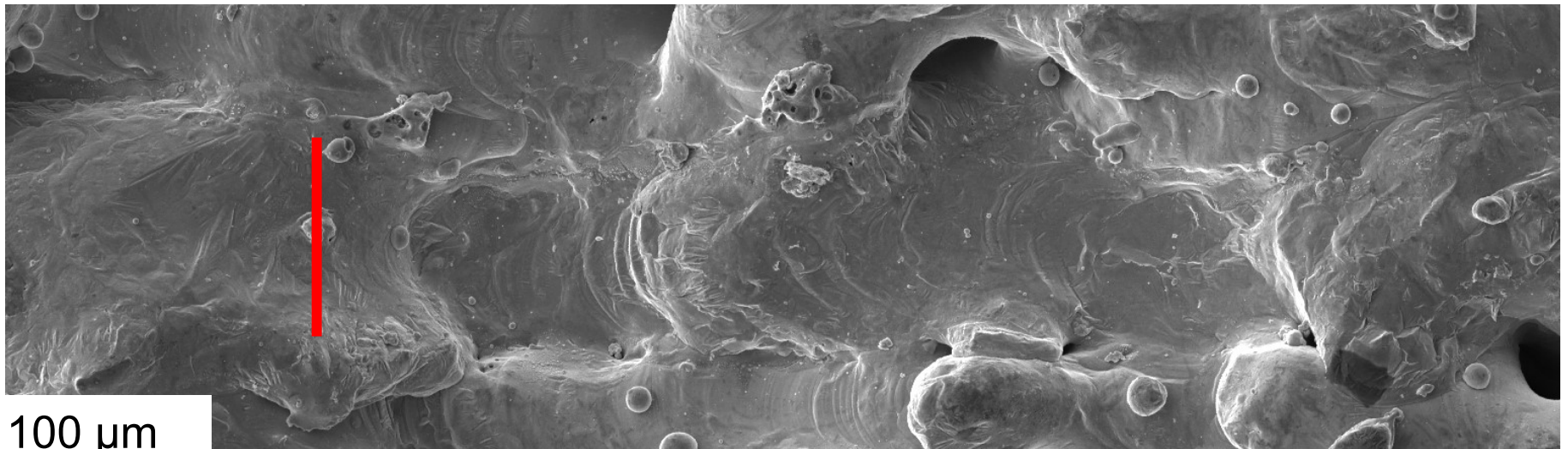
Goals

- Develop an analytical model to predict weld pool size.
- Demonstrate alloying success through analysis of the dispersoids produced via in situ AM.



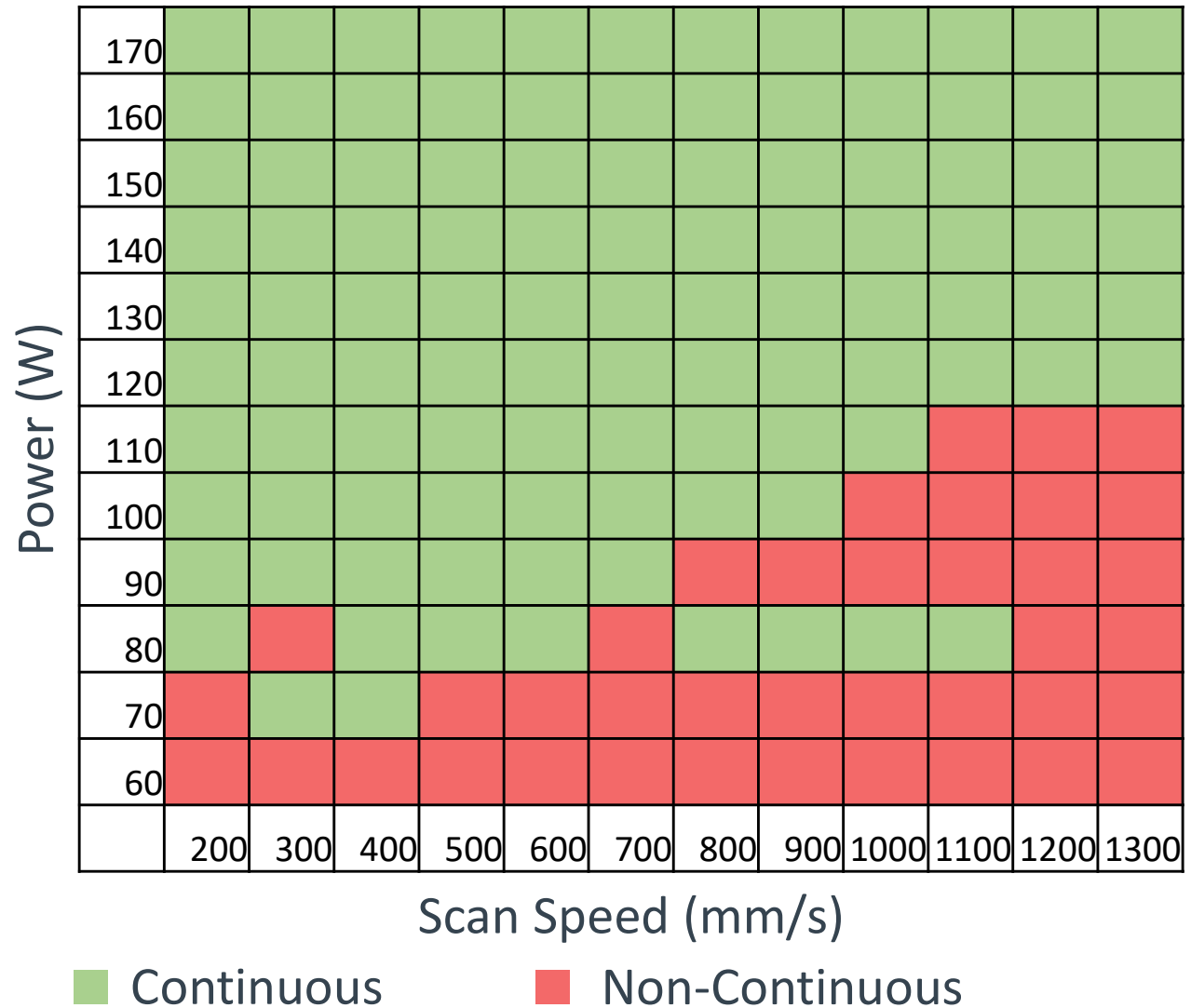
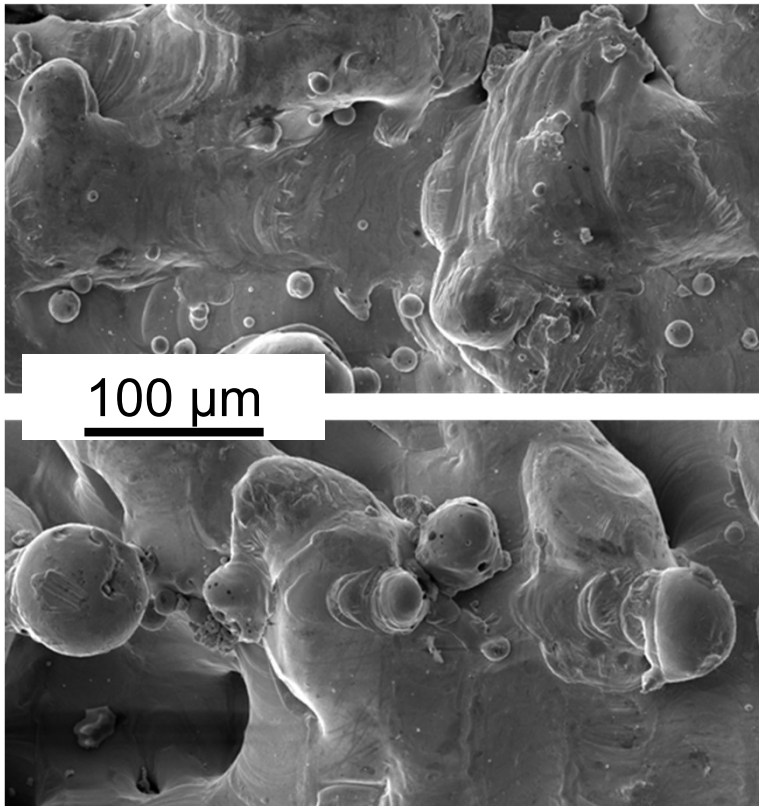
Single Track Measurements

- Single track scans build on larger AM blocks of the same material.
- Specimens in this study are highly porous, however fully dense specimens have been made and analysis is ongoing.
- Goal: For top-down data, **extract a width parameter from single track specimens.**



100 μm

Single Tracks – Linescan Continuity



Rosenthal Model

$$T(x, y, z) = T_0 + \frac{\alpha P}{2\pi\sigma\sqrt{(x - Vt)^2 + y^2 + z^2}} e^{\frac{-V\left(\sqrt{(x - Vt)^2 + y^2 + z^2} + (x - Vt)\right)}{2D}}$$

Assumptions:

- **Single point heat source**
- **No phase changes occur**
- **Isothermal properties**
- Heat is only conducted, no convection or radiation

Variables:

- (x, y, z) = coordinates with origin at the heat source (mm)
- P = Laser power (W)
- V = Laser velocity (mm/s)

Constants:

- T_0 = room temperature (or pre-heat temperature if using a heated plate, K)
- α = material absorptivity at laser wavelength
- σ = thermal conductivity (W / mm K)
- D = thermal diffusivity (mm² / s)

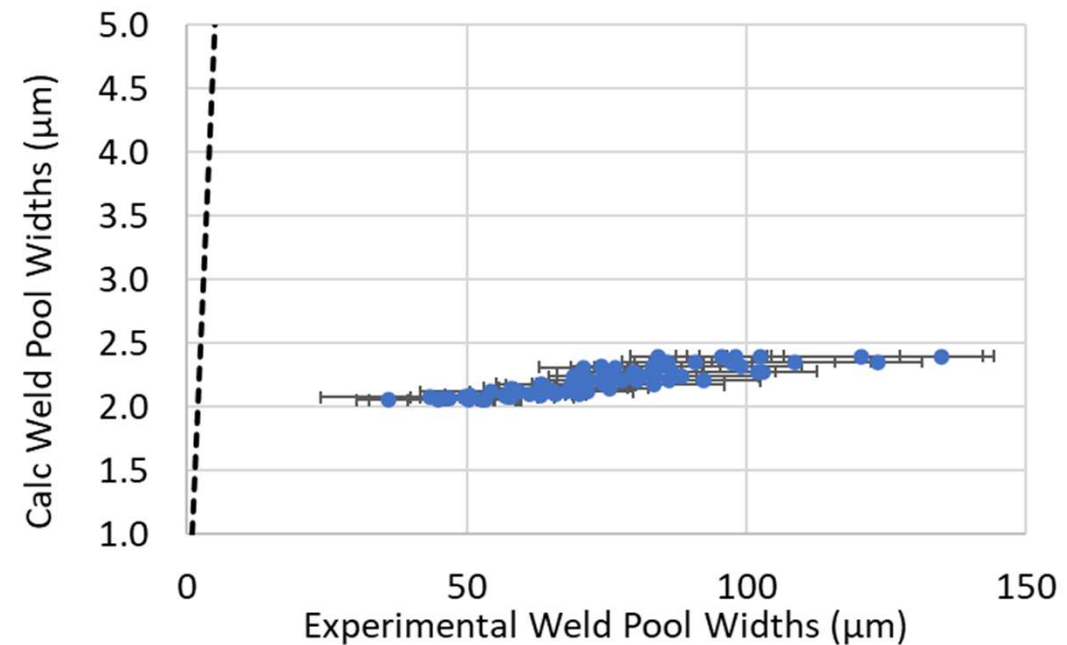
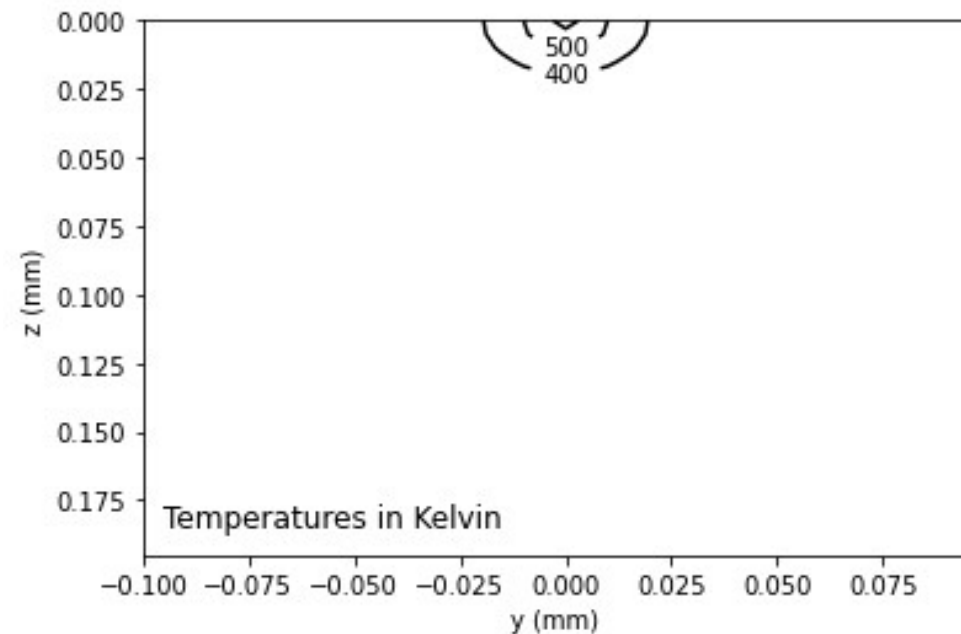
Rosenthal Model

$$T(x, y, z) = T_0 + \frac{\alpha P}{2\pi\sigma\sqrt{(x - Vt)^2 + y^2 + z^2}} e^{\frac{-V(\sqrt{(x - Vt)^2 + y^2 + z^2} + (x - Vt))}{2D}}$$

Advantages:

- Simple to code and understand
- Can be correlated with P&V of experimental data
- Already used in AM literature
- Not made for high conductivity materials
- Original Rosenthal assumptions need to be improved upon

Challenges:



Modifications to the Rosenthal Model

$$T(x, y, z) = T_0 + \frac{\alpha BP}{2\pi\sigma\sqrt{(x - Vt)^2 + y^2 + (Az)^2}} e^{\frac{-V(\sqrt{(x - Vt)^2 + y^2 + (Az)^2} + (x - Vt))}{2D}}$$

- Size and shape scalars:

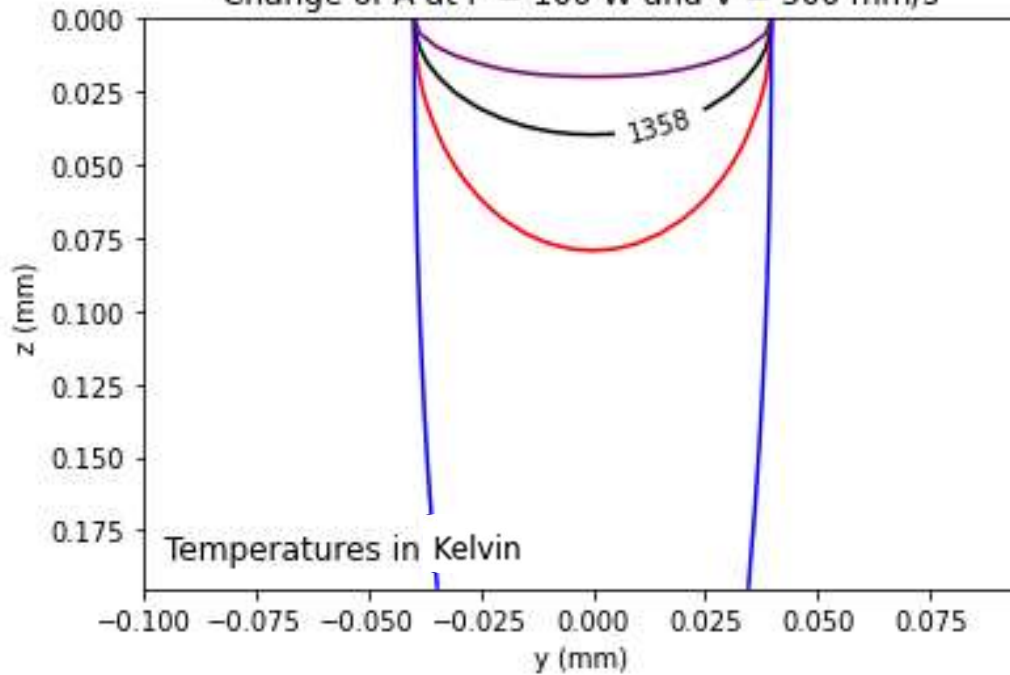
- A: Changes weld pool aspect ratio

A x0.1, x0.5, x1, x2

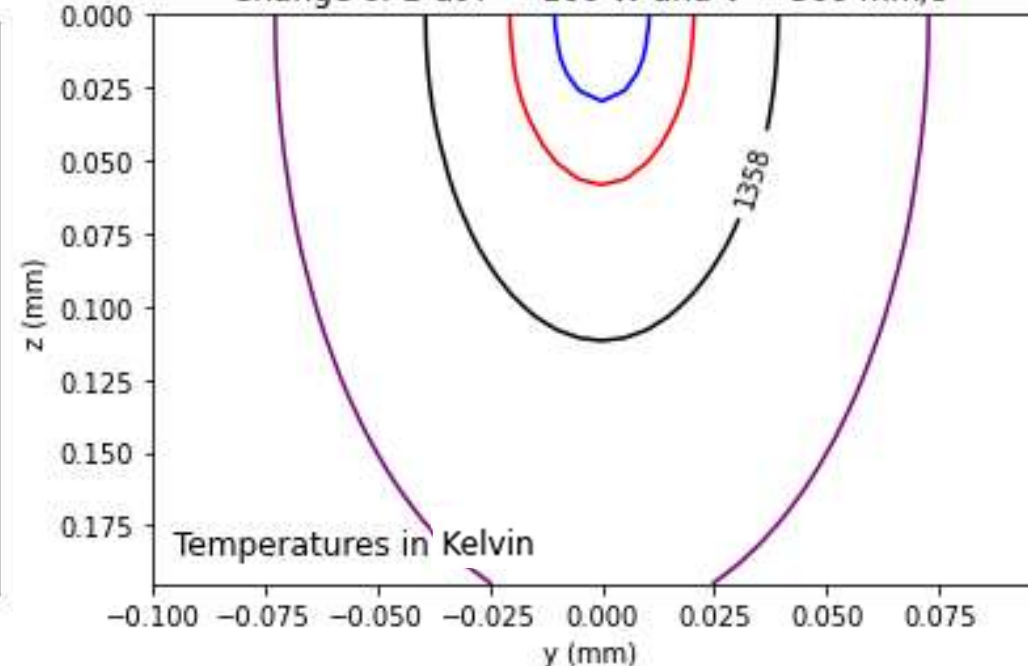
- B: scales weld pool

B x0.25, x0.5, x1, x2

Change of A at P = 100 W and V = 500 mm/s

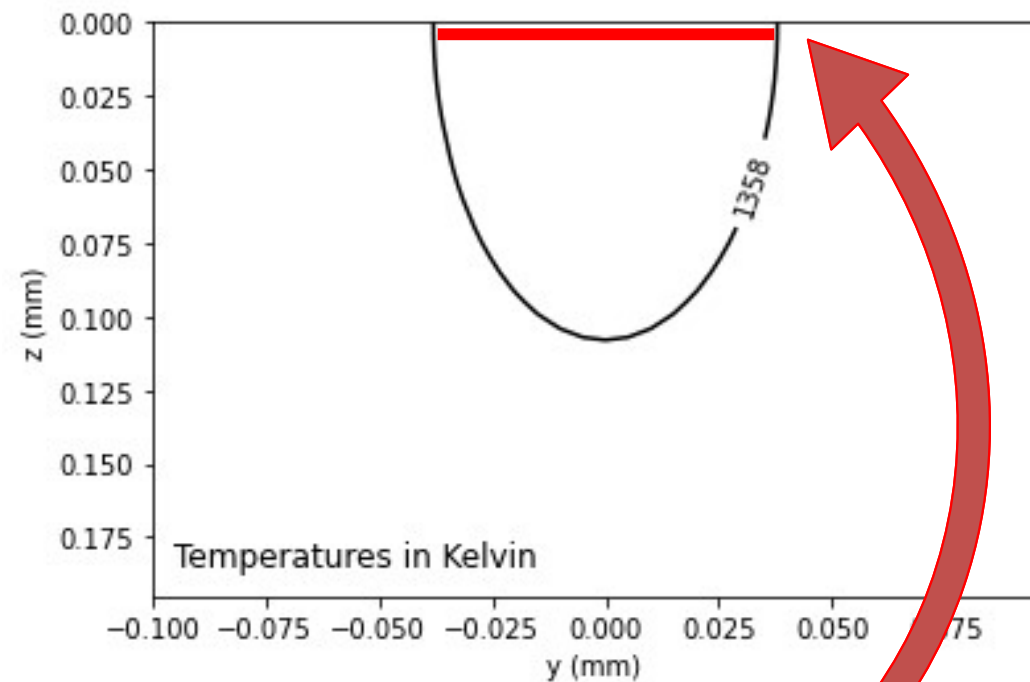
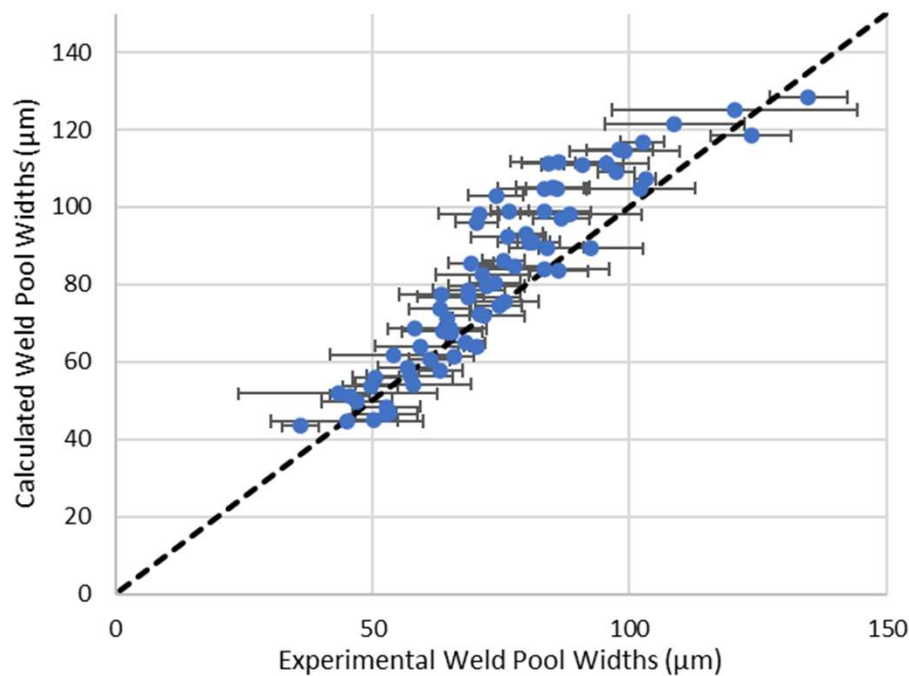


Change of B at P = 100 W and V = 500 mm/s

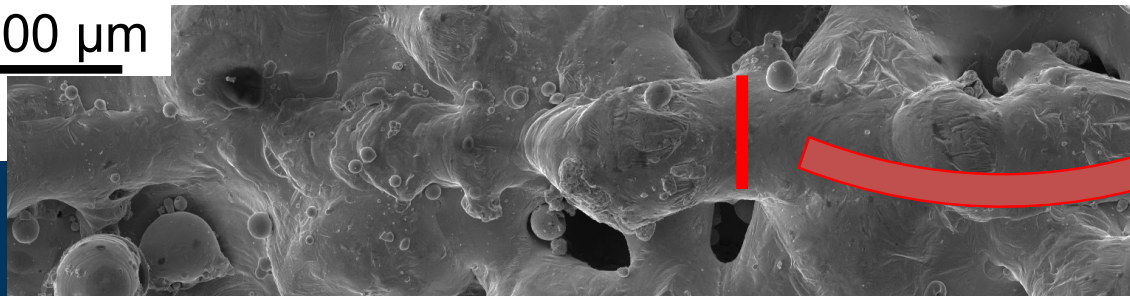


Measured Vs Calculated Widths

- Combining calculated widths and measured widths shows excellent agreement.
 - Dashed line is where $\text{width}_{\text{calc}} = \text{width}_{\text{meas}}$

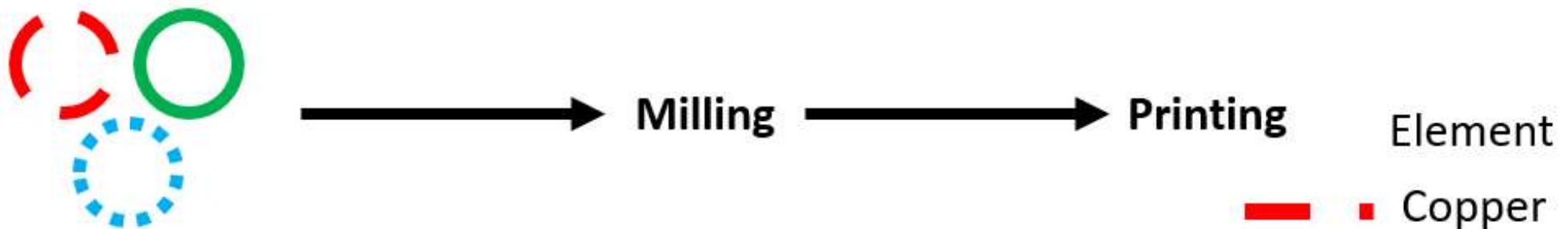


100 μm



Elemental Powder Preparation

One-Step Powder:

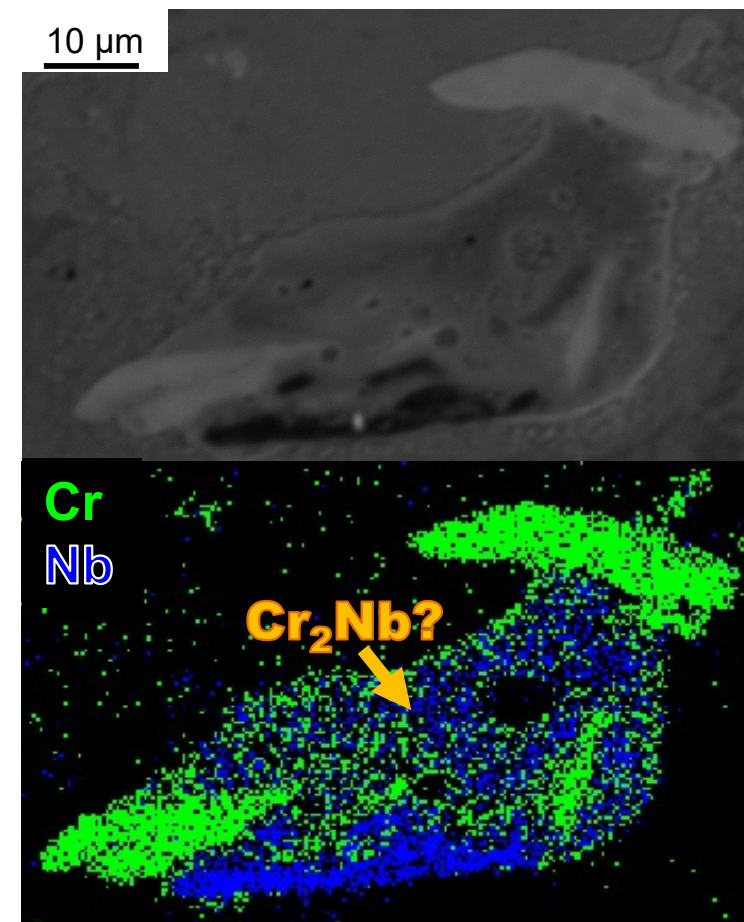
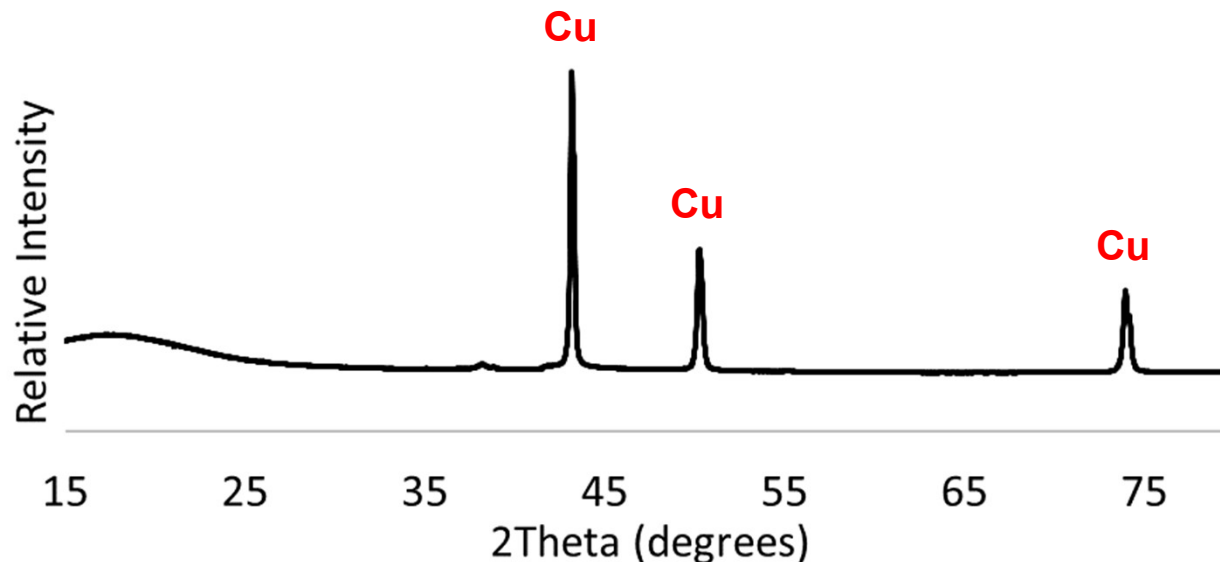


Two-Step Powder: creates more contact between Cr and Nb thus facilitating the formation of Cr_2Nb



Printed Components

- In situ alloying evident on metallographic sections.
 - Chromium (green) and niobium (blue).
 - EDS shows a mixture which suggests partially reacted Cr_2Nb
- Presence of Cr_2Nb not detected on XRD.
 - Cu peaks dominate XRD.
 - Cr_2Nb is below detection limit in bulk sample.

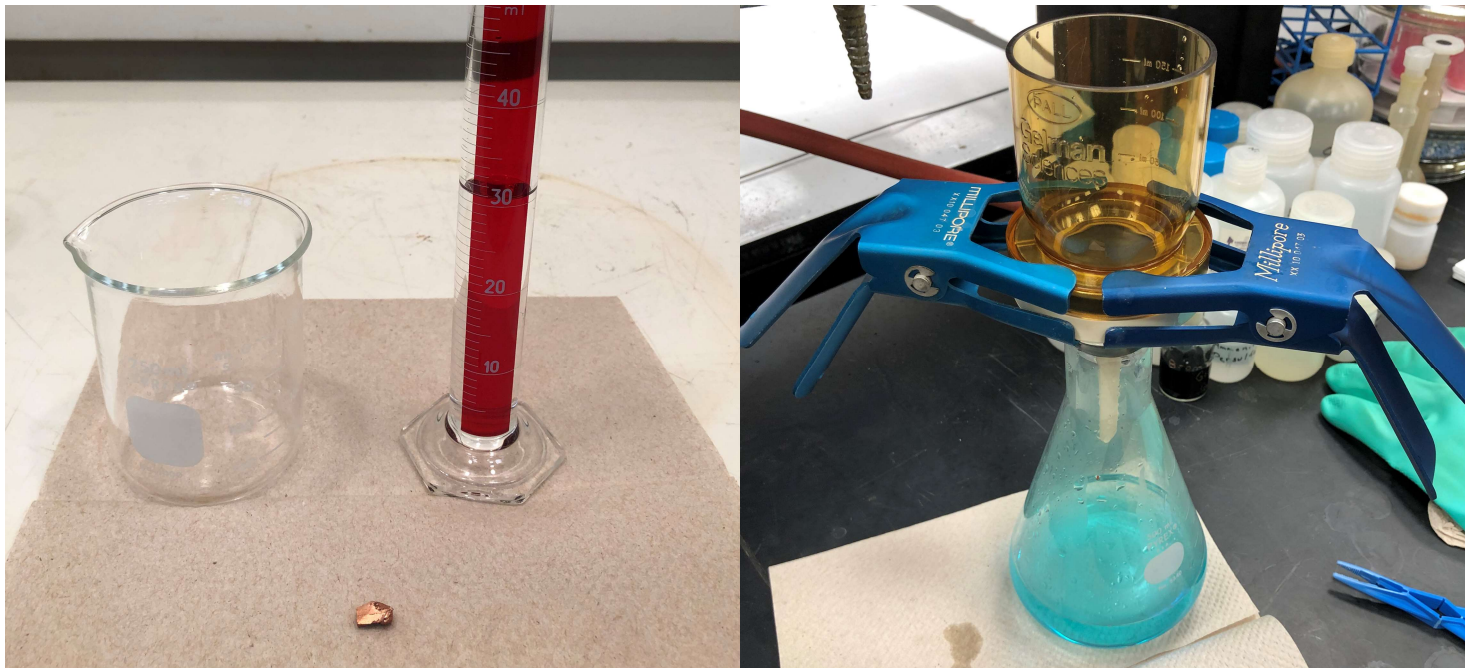
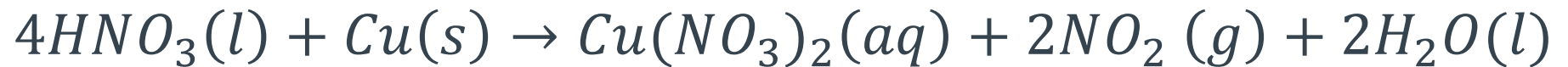


⁴ D. Scannapieco, CWRU Senior Thesis, 2019.

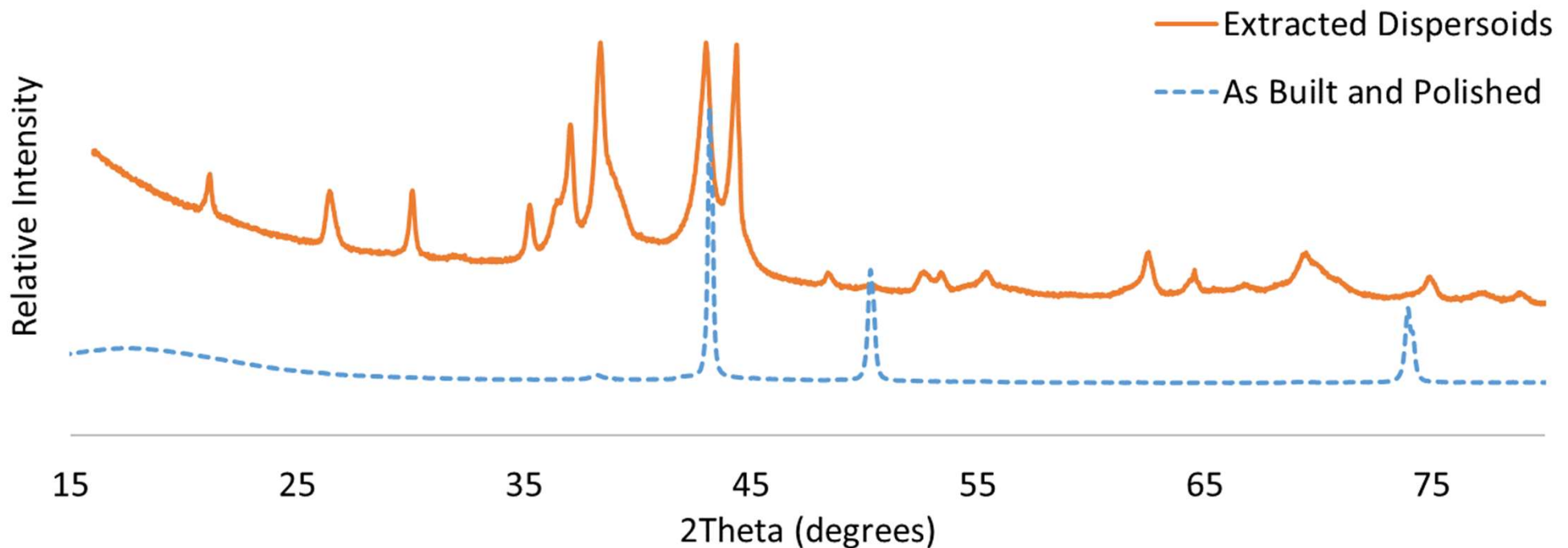


Phase Extraction of Dispersoids

- To eliminate Cu from XRD consideration, extract out the Cr_2Nb dispersoids.
- Nitric acid is nonreactive with Cr, Nb, Cr_2Nb , and associated oxides.
 - Nitric Acid does dissolve Cu.

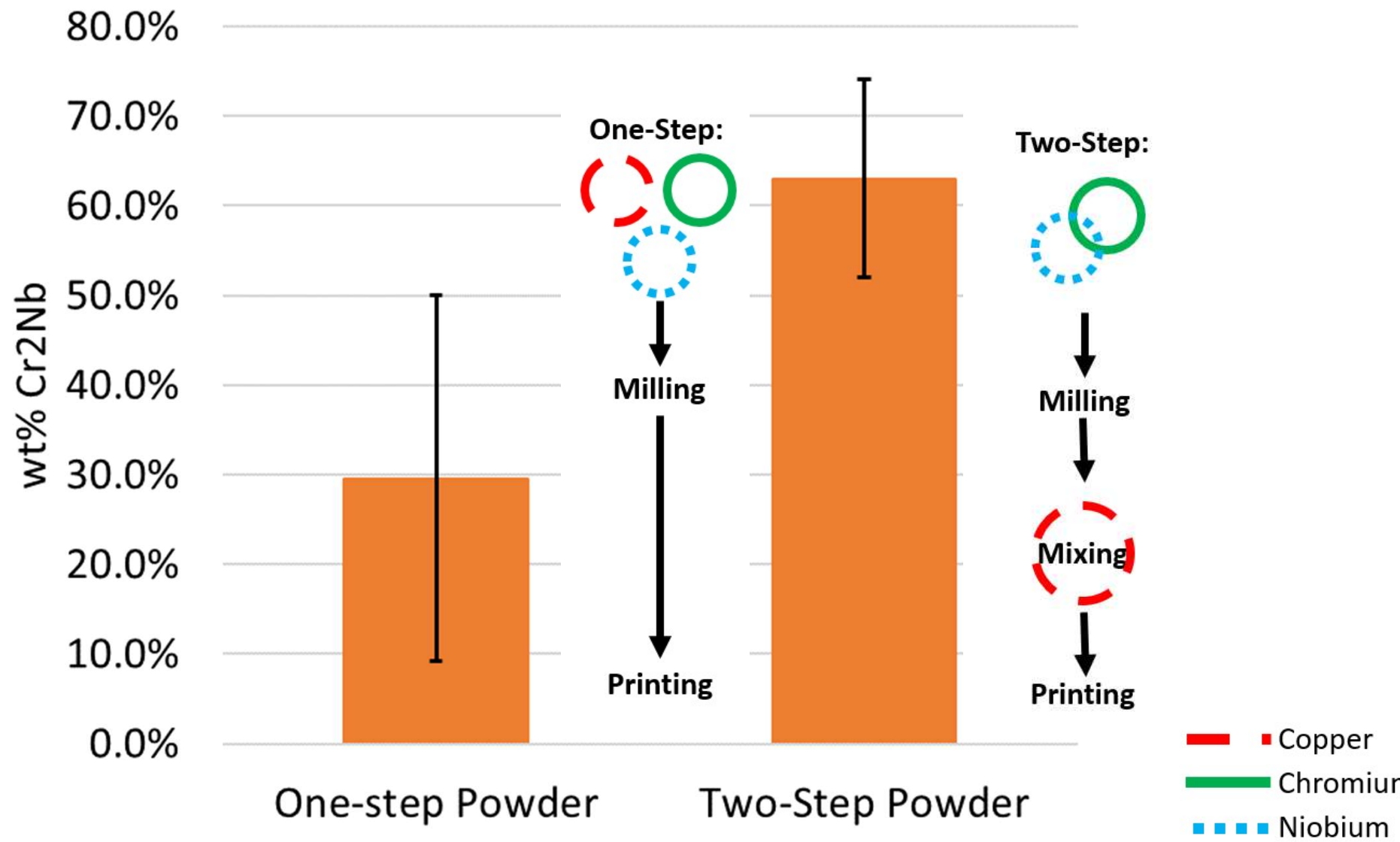


Phase Extraction of Dispersoid



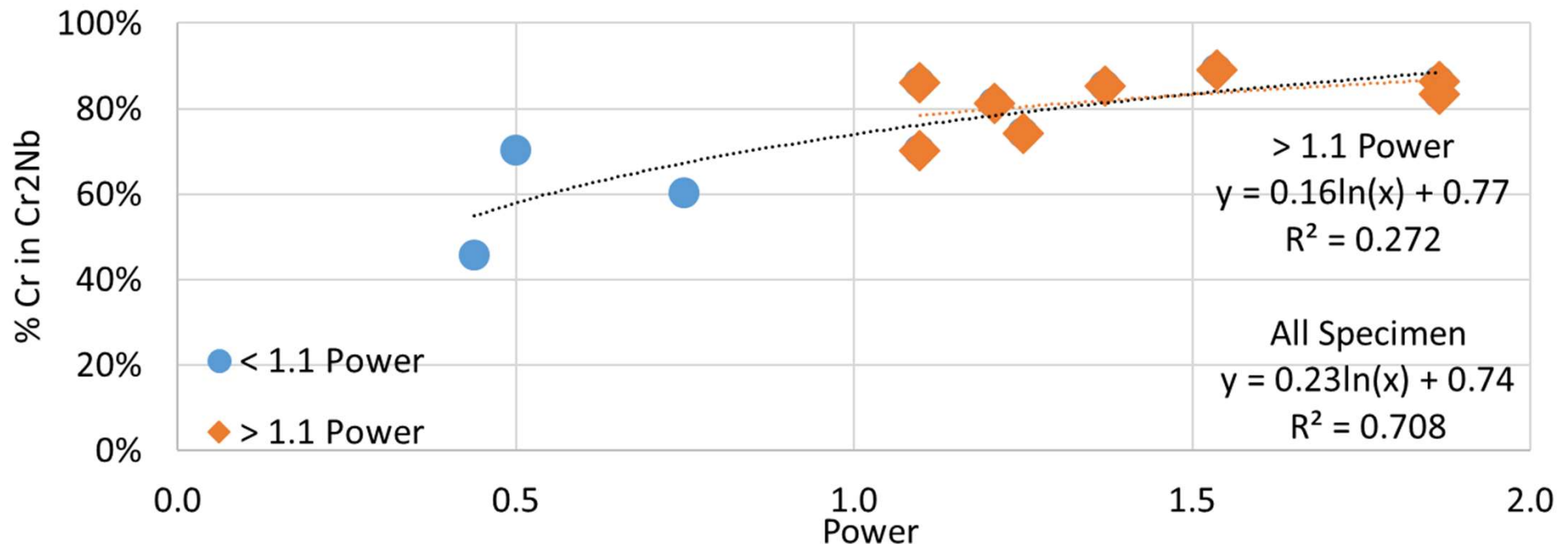
- Phase extraction reveals presence of Cr_2Nb .
 - Dispersoids total 7 vol% of alloy.
- Can now identify differences in success of conversion to Cr_2Nb .

Milling Impact on Cr₂Nb Conversion



⁶ D. Scannapieco, et al. NASA/TM-20205003857, June 2020.

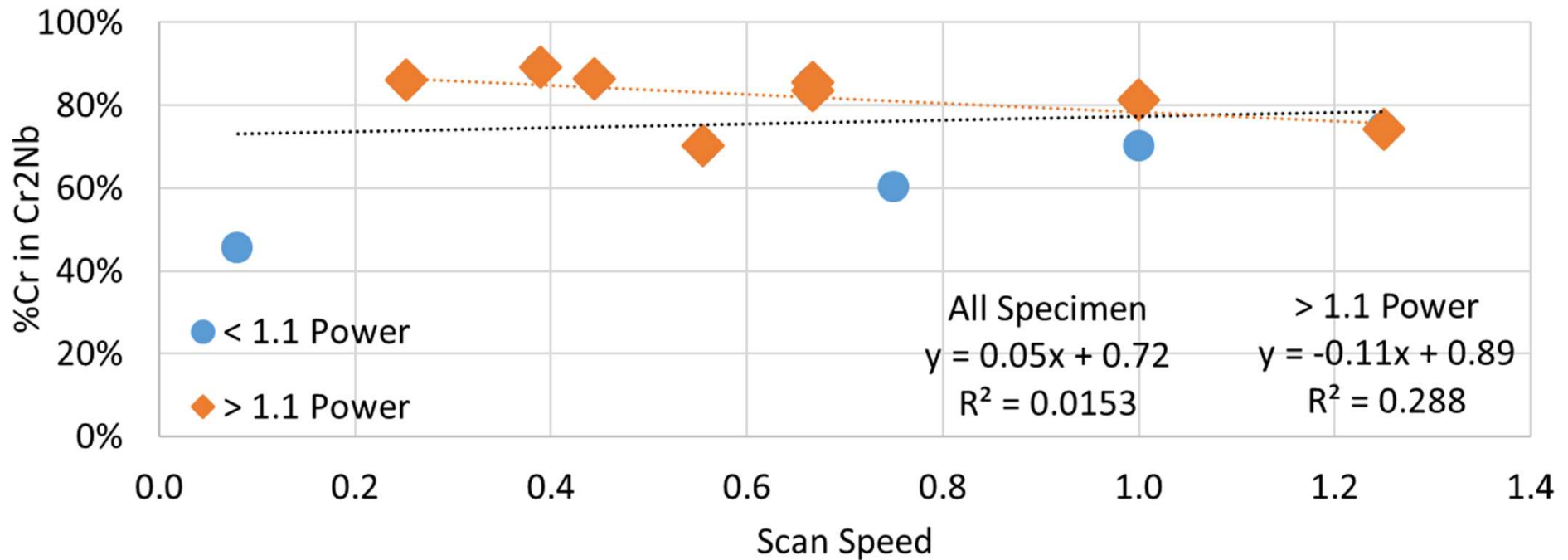
Laser Power Impact on Cr₂Nb Conversion



- %Cr in Cr₂Nb trends positively with laser power.
- Clear distinction in laser power benefit above and below 1.1 power.
 - Suggests a minimum of 1.1 power is needed for high Cr₂Nb conversion.
 - Addition power above that is not an efficient means of promoting the reaction.

⁶ D. Scannapieco, et al. NASA/TM-20205003857, June 2020.

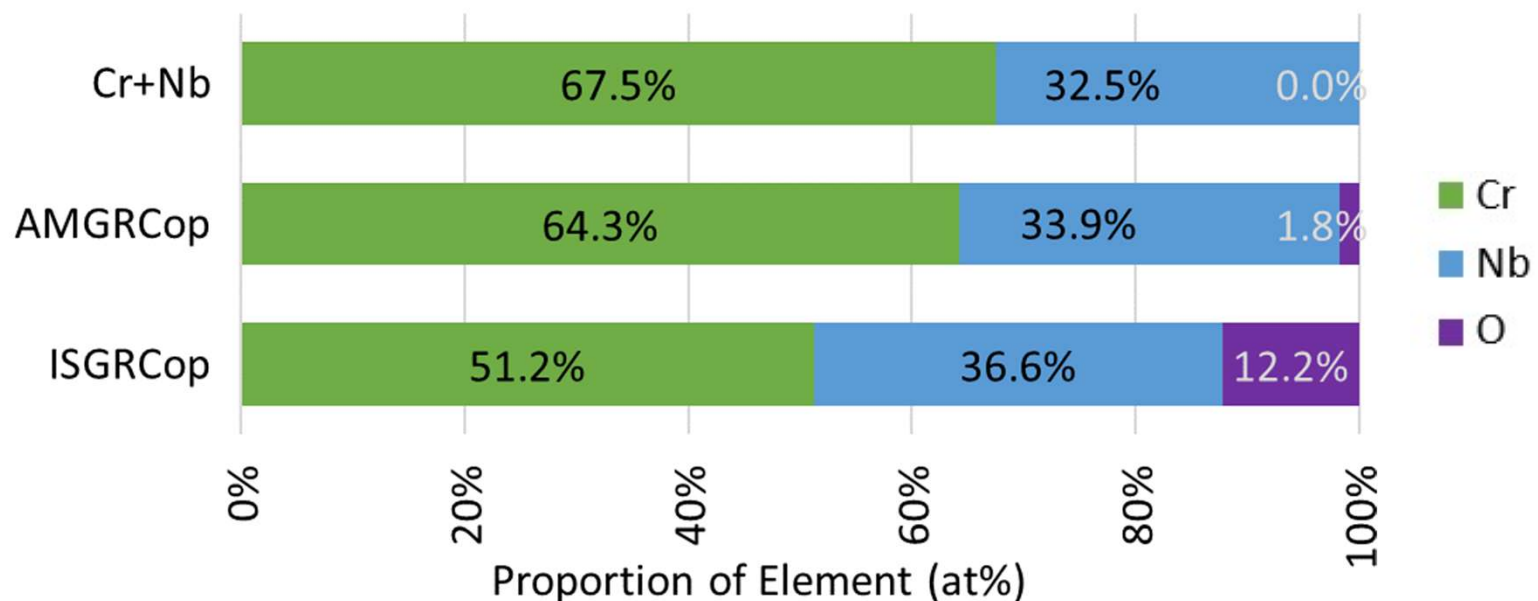
Laser Scan Speed Impact on Cr₂Nb Conversion



- Influence of scan speed on in situ alloying success is negligible.

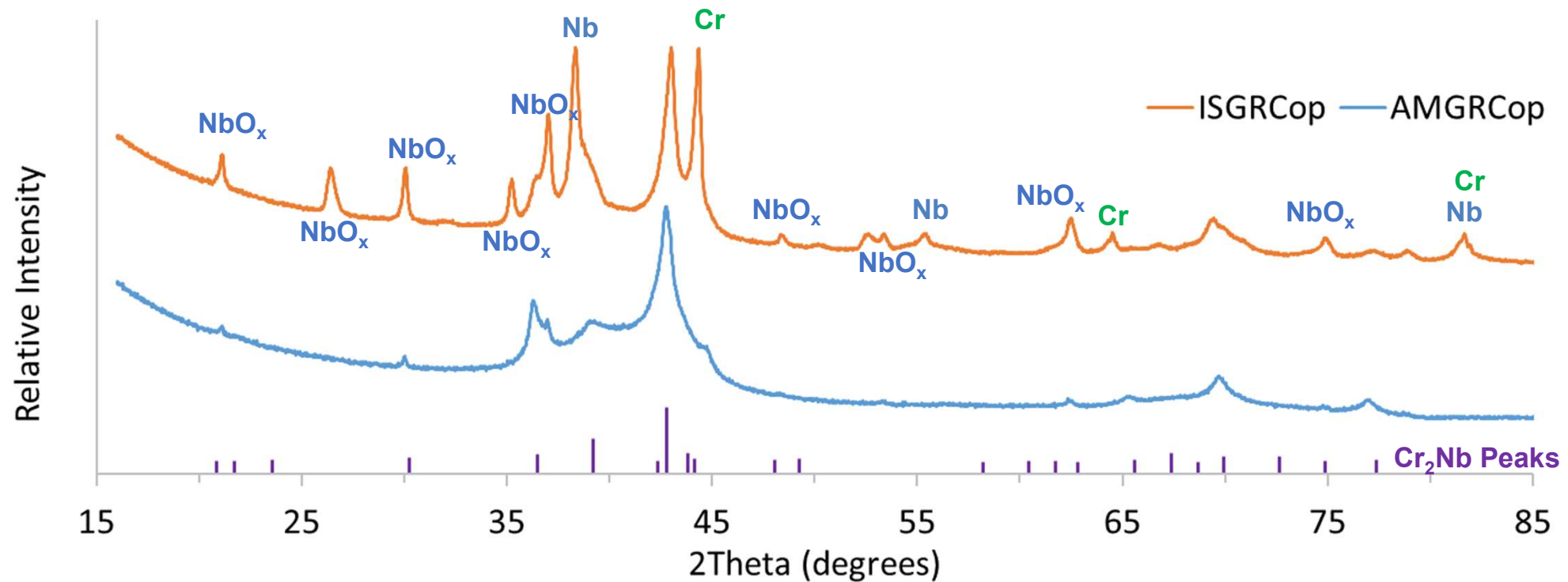
Processing Impact on Extracted Dispersoid Chemistry

- Powder (Cr+Nb) is oxygen free and Cr-rich, 2.08:1 Cr:Nb ratio.
- Both conventional AM and ISGRCop have oxygen, and are Nb-rich.
 - AM is 1.90:1 Cr:Nb ratio.
 - ISGRCop 1.40:1 Cr:Nb ratio, after starting with the 2.08:1 powder.
- No oxides detected in starting powders.



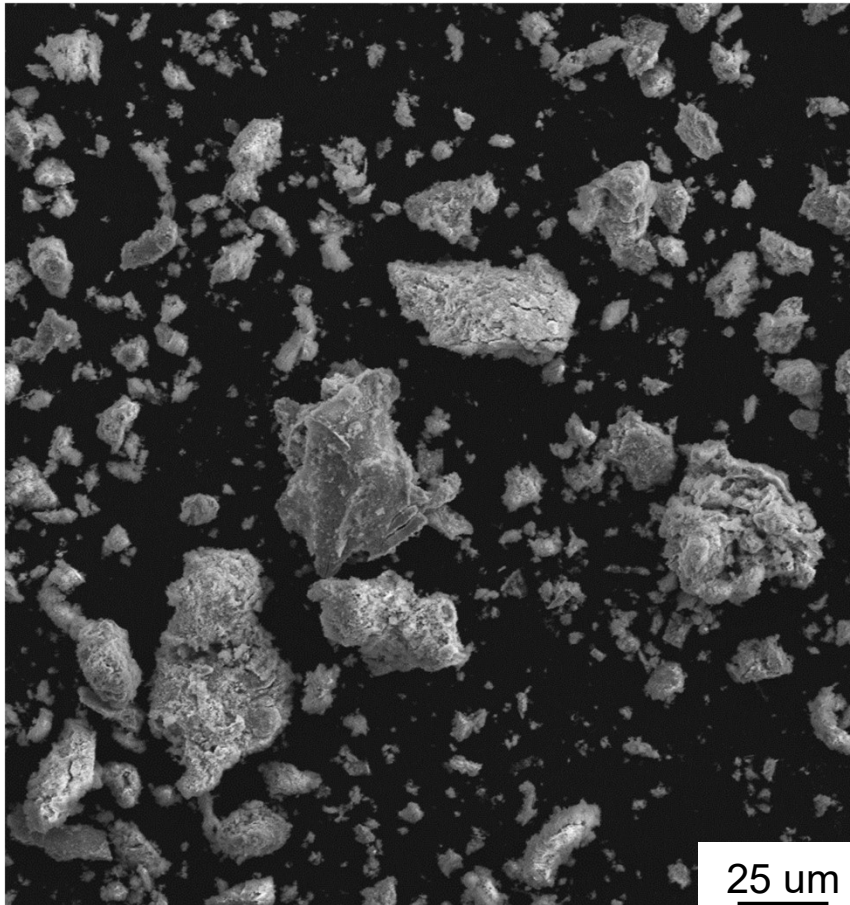
Processing Impact on Extracted Dispersoid Phases

- Extraneous peaks on ISGRCop line are primarily Nb-based oxides.
 - Very high oxygen content in ISGRCop dispersoids has an uncertain origin.
 - EOS M100 operates at < 0.1% Oxygen in the chamber.

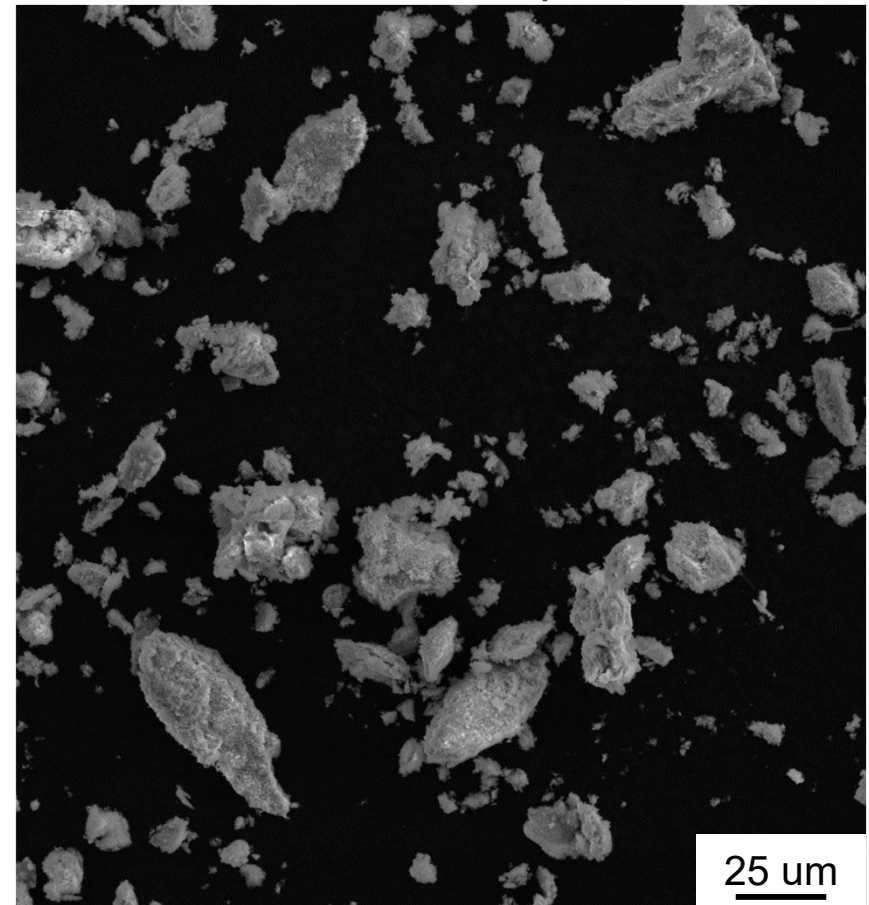


Processing Impact on Extracted Dispersoid Morphology

ISGRCop

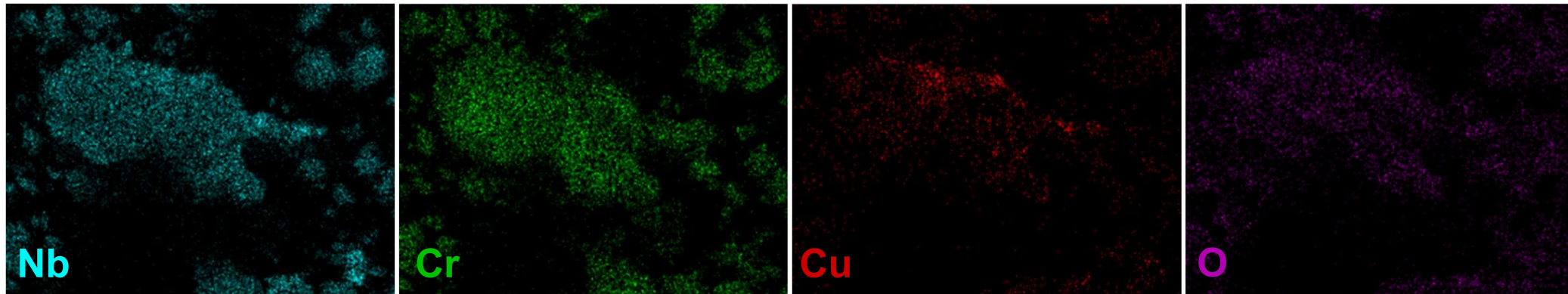


AMGRCop

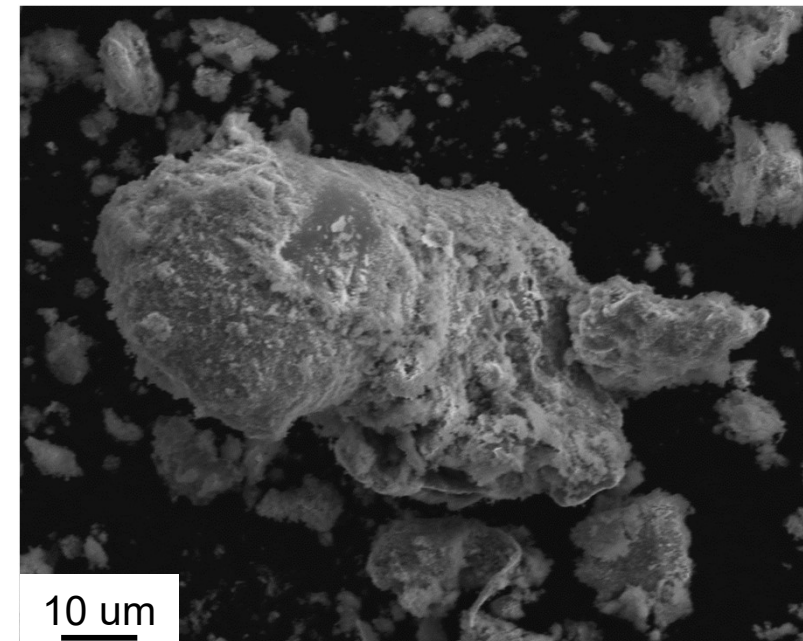


- Morphologies are similar between alloys.
- Suggesting that their mechanical strengthening effect will be similar.

Extracted Precipitate Chemistry



- Extensive overlap of Cr and Nb EDS maps
- Little to no elemental segregation observed.
 - Several phases of each element is found on each particle.
 - No apparent concentration of oxides.
- Similar mappings are found in other samples.
- Trace amounts of Cu detected, despite no XRD evidence of Cu in these specimens.



Conclusions

- An analytical model to predict weld pool size of in situ alloyed GRCo-42 during additive manufacturing has been developed.
 - The model shows promising agreement with experimental top-down width measurements.
- Powder preparation methods show strong correlation with the in situ alloying success rate.
 - Two-step processed powder greatly increases the alloying success and consistency.
- A minimum normalized laser power of 1.1 was discovered as for optimum in situ alloying success.
 - Laser velocity was not found to significantly influence alloying success.
- Morphology and chemical distribution of the dispersoids was found to be similar between in situ alloyed GRCo-42 and conventionally manufactured GRCo-42.

Acknowledgements

Support is provided by NASA Grant NASA-80NSSC19K1736 ‘In-situ alloying of GRCop-42’, NASA ULI: NASA-80NSSC19M0123 ‘Development of an Ecosystem for Qualification of AM Processes and Materials in Aviation’, and CWRU’s Arthur P. Armington Professorship.

Additionally, this work would not be possible without our excellent colleagues at:

NASA GRC

Dereck Johnson
Aaron Thompson
Wayne Jennings
Joy Buehler
Laura Evans
Pete Bonacuse
Cheryl Bowman
Richard Rogers
Gustavo Costa

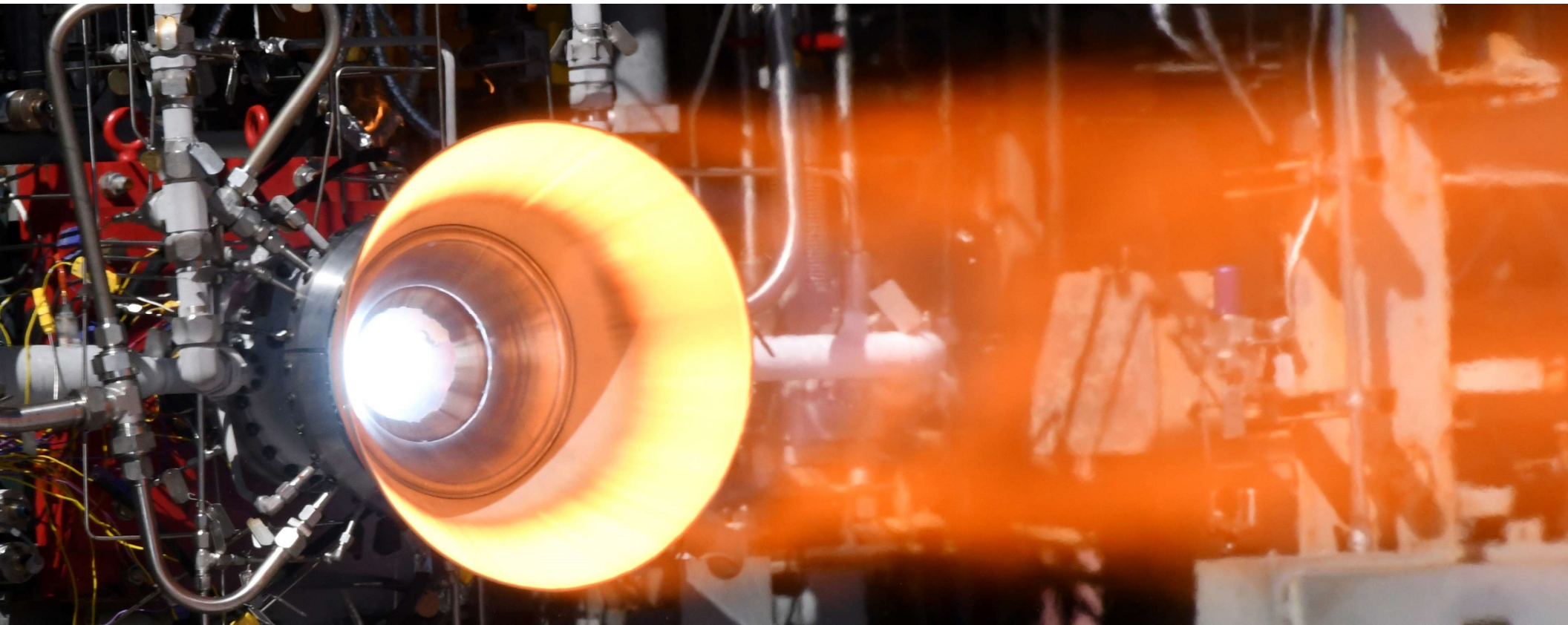
NASA MSFC

Paul Gradl
Chris Protz
John Fikes
Parker Shane
Tim Poe

CWRU

Jackson Smith
Jennifer Carter
Rich Tomazin

CMU Led NASA ULI



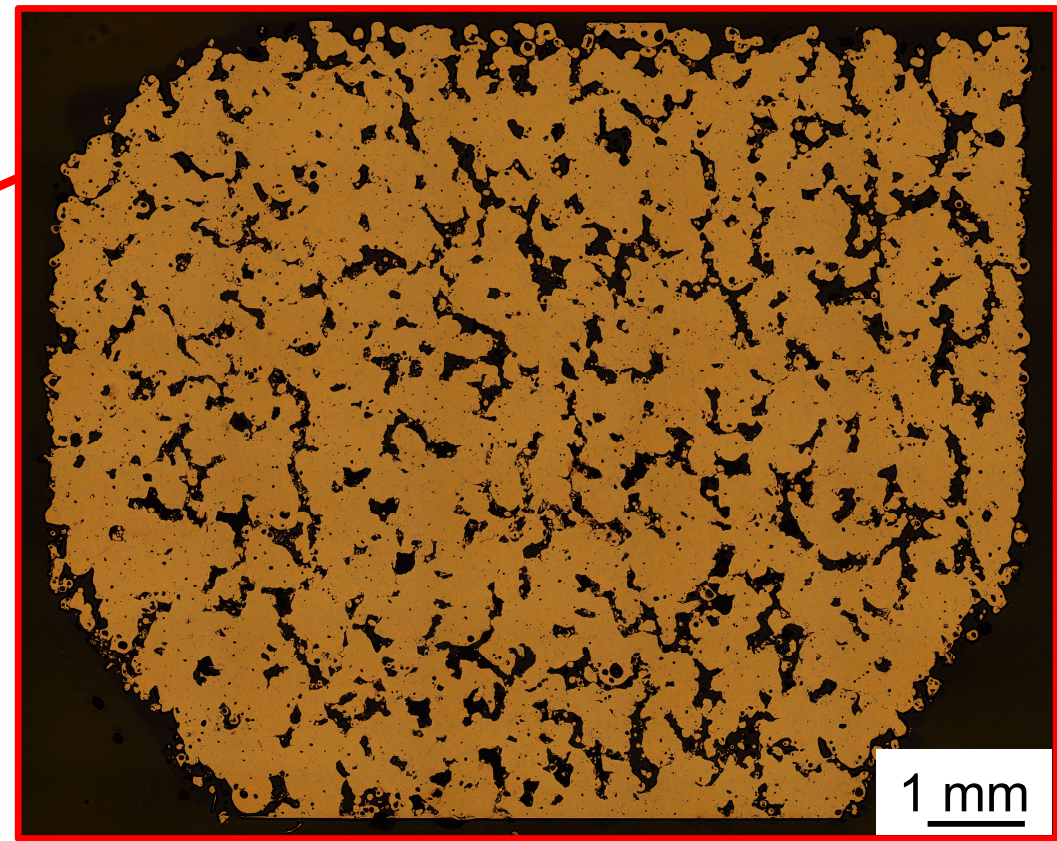
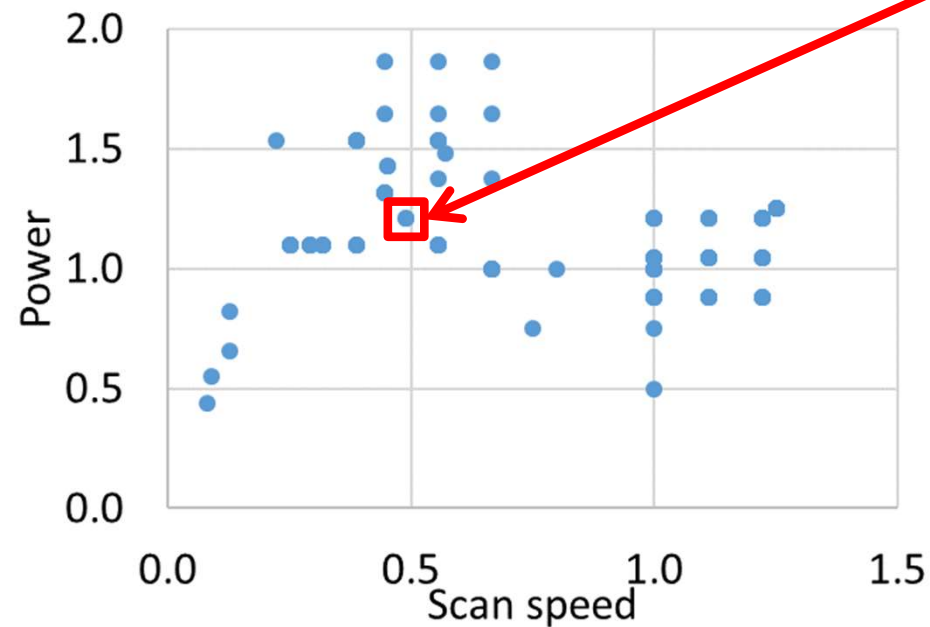
Questions?

References

1. A. Grigoriev, I. Polozov, V. Sufiiarov, and A. Popovich, "In-situ synthesis of Ti_2AlNb -based intermetallic alloy by selective laser melting". J. Alloys Compd, Vol 704, p 434-442, 2017.
2. K. G. Cooper, J. L. Lydon, M. D. LeCorre, Z. C. Jones, D. S. Scannapieco, D. L. Ellis and B. A. Lerch, "Three dimensional printing of GRCo-42," *NASA TM 2018220129*, 2018.
3. D. L. Ellis, "GRCo-84: A High-Temperature Copper Alloy for High-Heat-Flux Applications," NASA TM - 2005-213566, 2005.
4. D. S. Scannapieco, "Additive Manufacturing of GRCo-42" CWRU, Senior Thesis, April 2019.
5. L. R. Summerlin, C. L. Borgford, and J. B. Ealy, "Ira Remsen's Investigation of Nitric Acid," *Chemical Demonstrations: A Sourcebook for Teachers Vol. 2*, Washington D.C., American Chemical Society, 1987, pp 4-5.
6. D. Scannapieco, R. Rogers, D. Ellis, and J. Lewandowski, "In-Situ Alloying of GRCo-42 via Additive Manufacturing: Precipitate Analysis" NASA/TM-20205003857, June 2020.

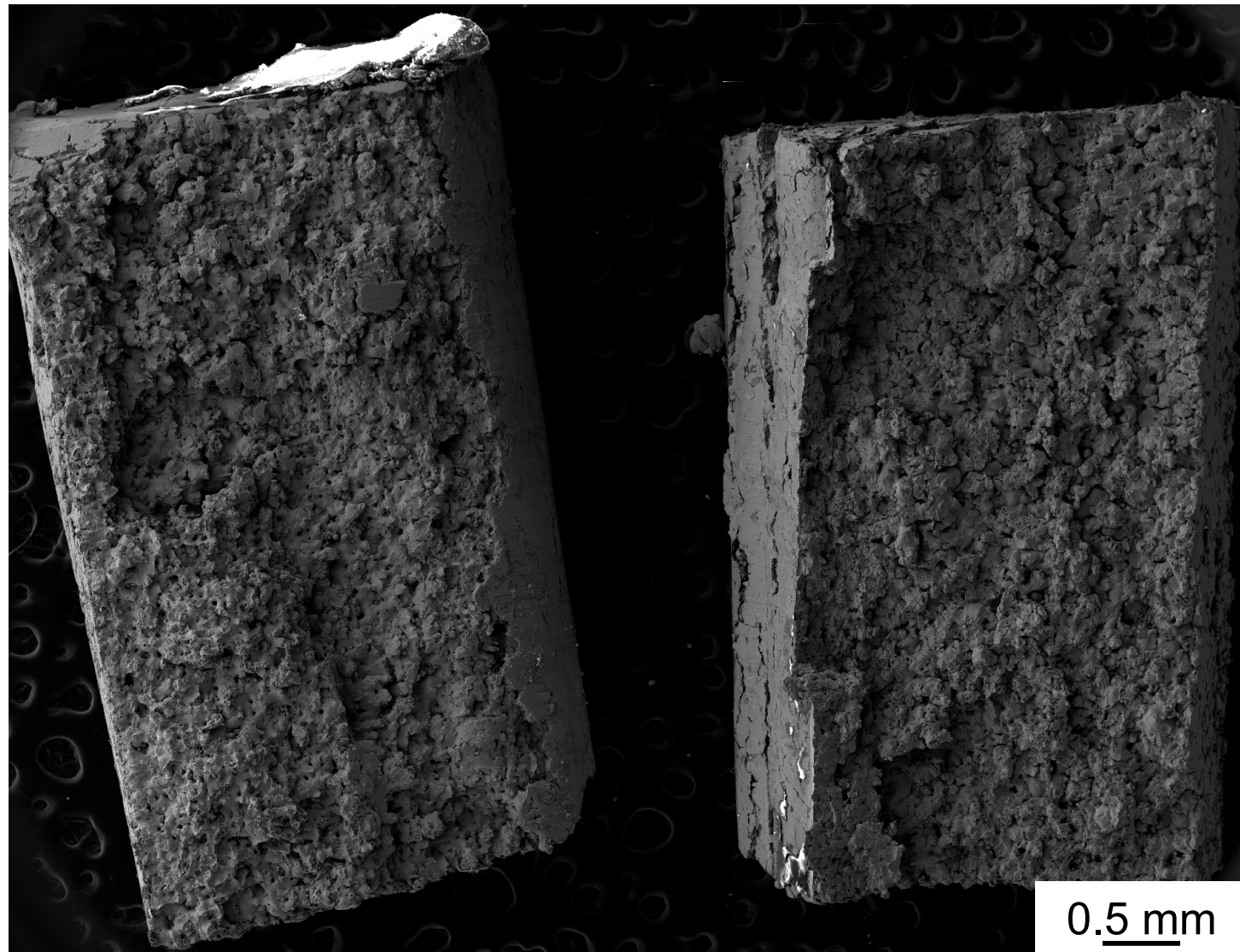
Parameter Mapping

- High porosity detected in the printed materials.
- Cu has high reflectivity in 1064 nm wavelength used by EOS M100.
- Best density was 95%, which is too high to HIP out and retain dimensional fidelity.



Fractography to Image Porosity Details

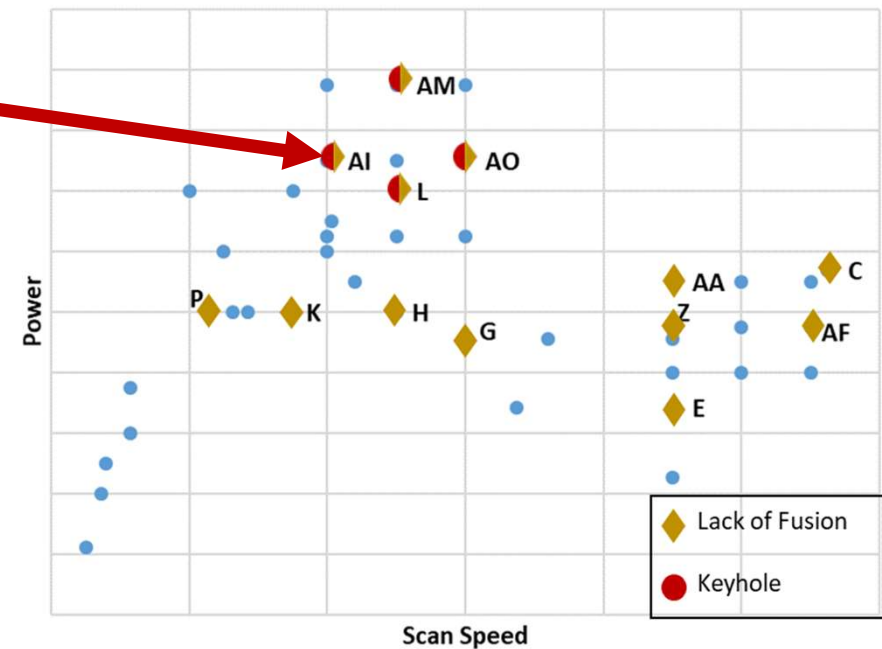
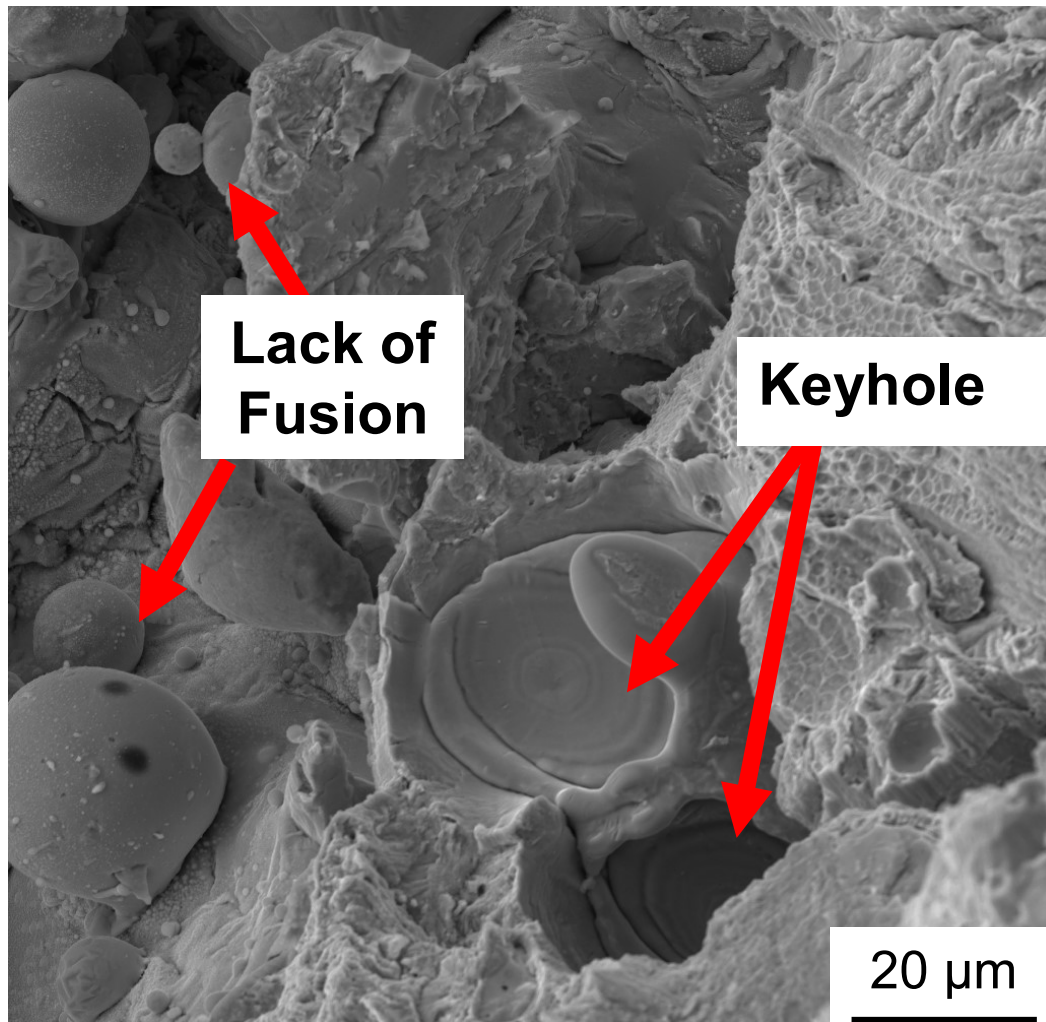
- Fatigue provides fracture surfaces with unique lack of fusion and keyhole defects.
- These defects can provide insight on what needs to change to optimize the parameters.



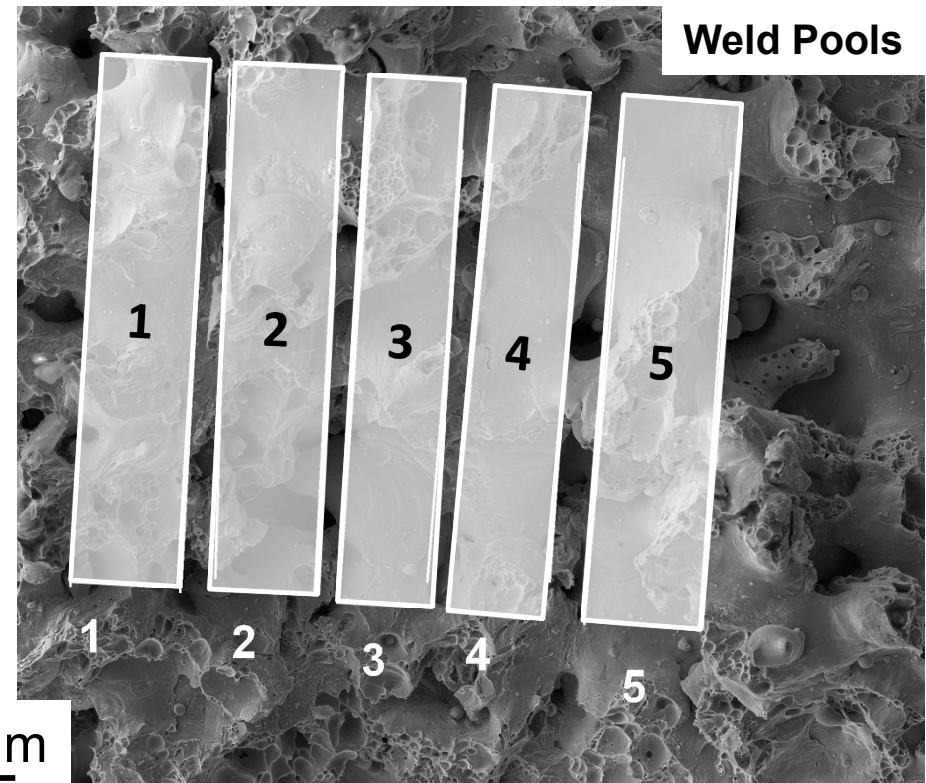
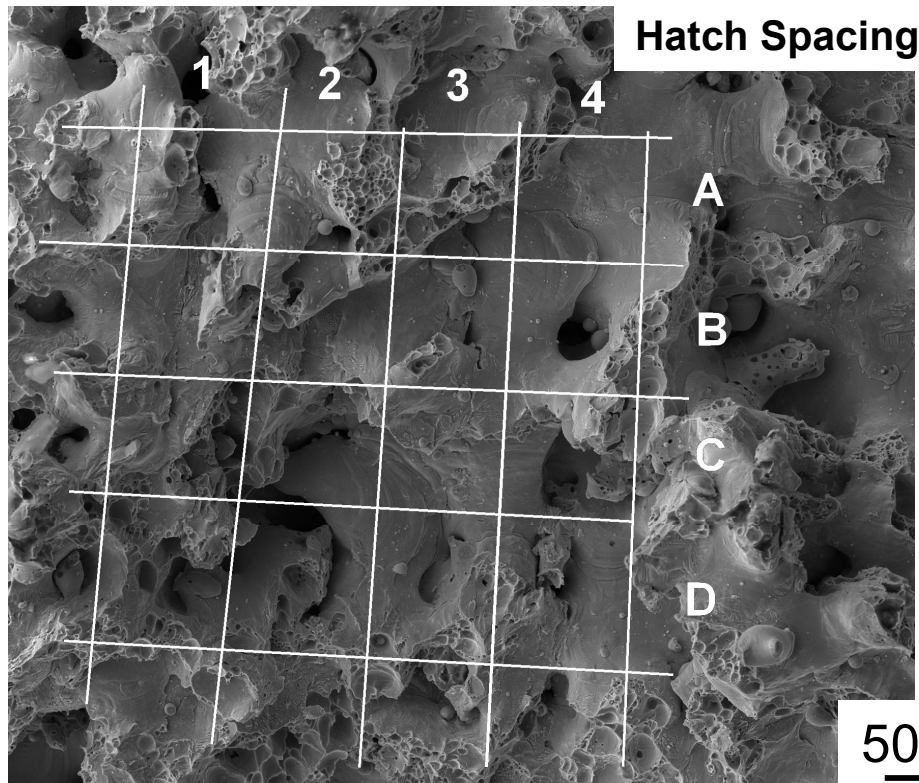
0.5 mm



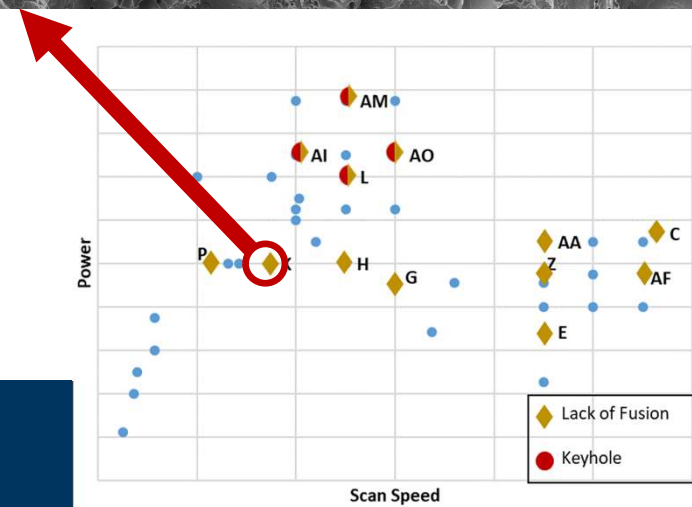
Fractography to Image Porosity Details



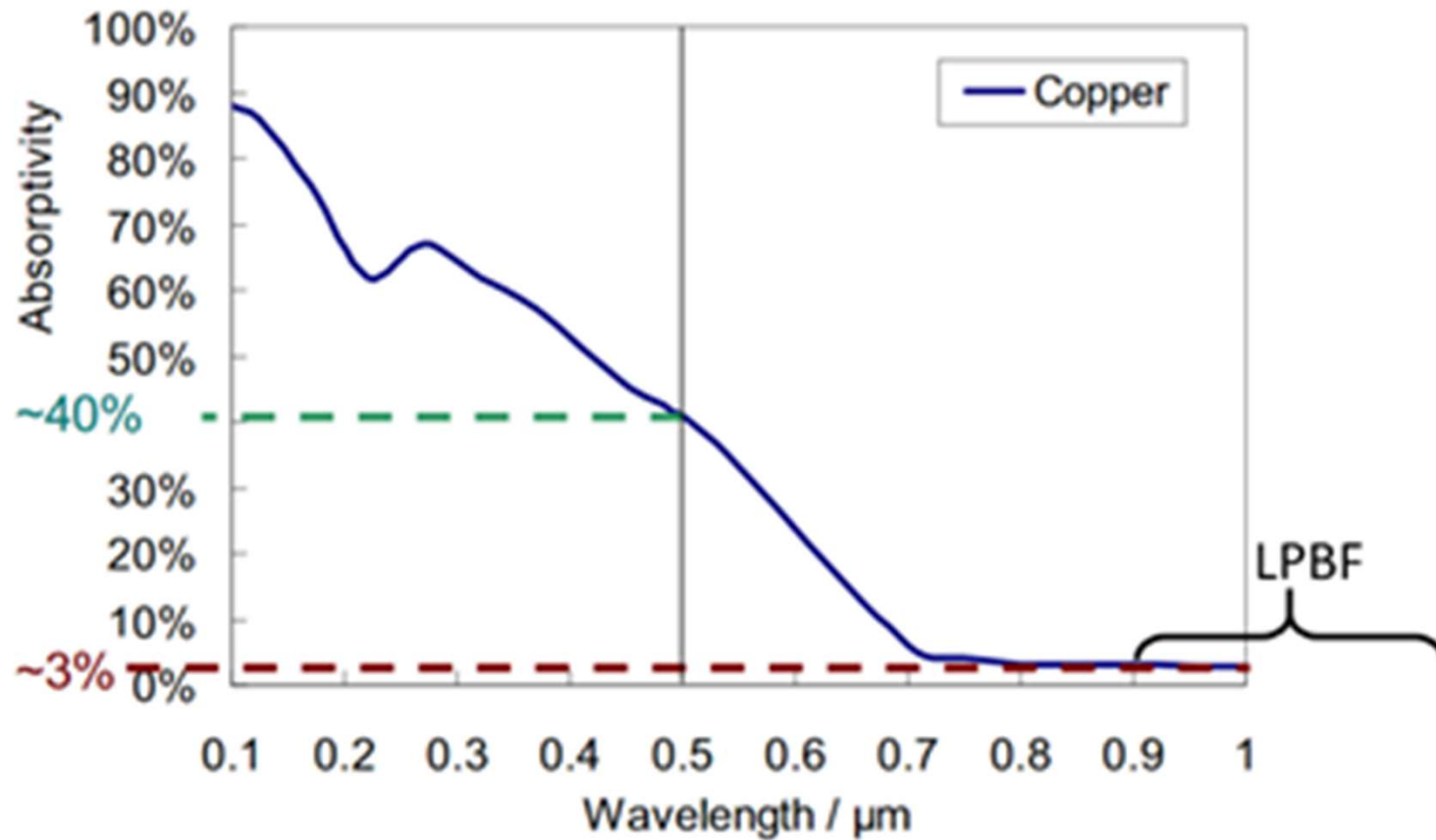
Fractography to Image Porosity Details



- Hatch spacing ($72\text{ }\mu\text{m}$) > Weld pool ($56\text{ }\mu\text{m}$)
 - Creates lack of fusion at any P-V combination



- Hess et al. Physics Procedia (2010).



Hess et al. Physics Procedia (2010)

Precipitate Phase ID (wt%)

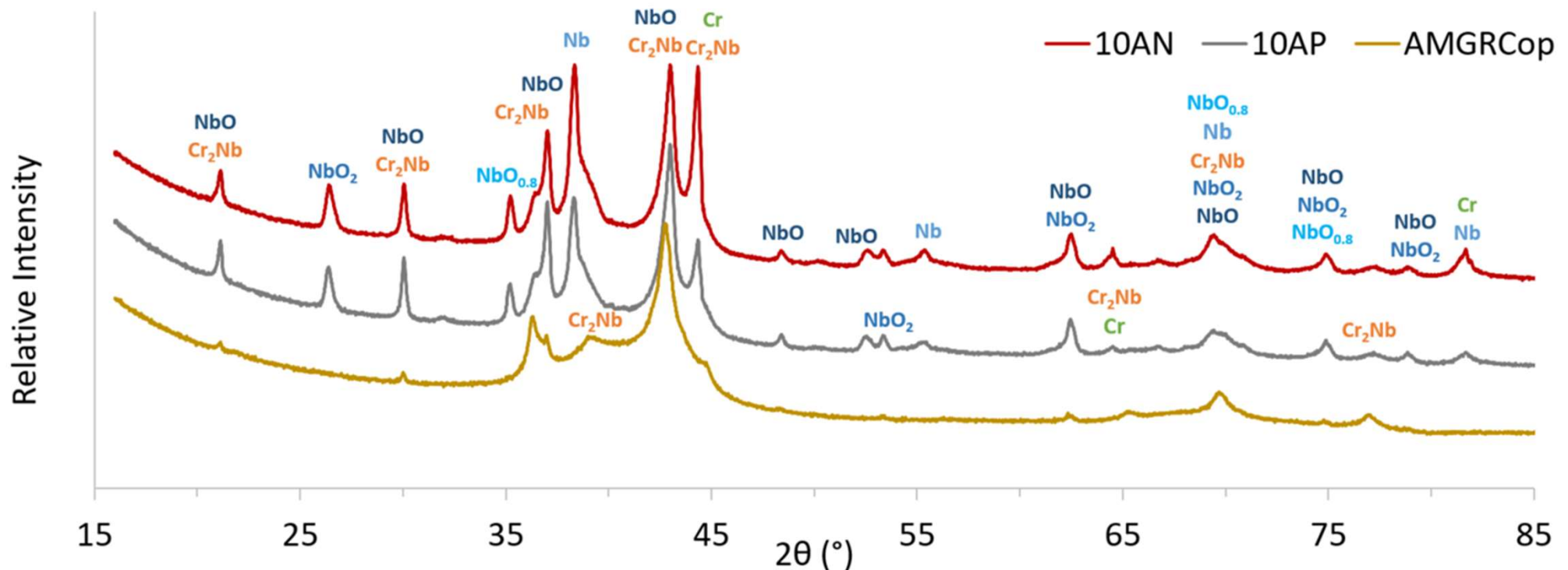
Specimen	Nb	Cr2Nb	NbO	NbO2	Cr	NbO0.8	Cu
01F	58.7%	14.7%	2.4%	5.1%	3.3%	2.0%	13.8%
01B	58.4%	20.3%	5.6%	12.1%	3.5%	0.0%	0.0%
03J	55.1%	15.6%	16.3%	12.1%	1.0%	0.0%	0.0%
05H	25.0%	53.7%	3.6%	2.3%	12.0%	3.3%	0.0%
05P	7.4%	71.3%	8.6%	3.8%	6.1%	2.7%	0.0%
05U	18.0%	38.5%	1.4%	3.5%	24.3%	3.5%	10.8%
07AA	12.3%	70.3%	5.9%	2.9%	8.6%	0.0%	0.0%
08C	15.7%	64.7%	5.2%	2.6%	11.8%	0.0%	0.0%
10AJ	3.1%	67.1%	18.0%	6.2%	5.6%	0.0%	0.0%
10AN	7.6%	75.4%	6.8%	3.4%	6.8%	0.0%	0.0%
10AP	10.5%	63.2%	15.7%	3.9%	6.6%	0.0%	0.0%
AM	0.0%	97.0%	3.0%	0.0%	0.0%	0.0%	0.0%
Cr+Nb	46.2%	0.0%	0.0%	0.0%	53.8%	0.0%	0.0%

Precipitate Chemistry (at%)

Specimen	Nb	Cr	O	Cu
01F	58.8%	15.9%	8.9%	16.5%
01B	62.9%	19.6%	17.5%	0.0%
03J	63.8%	12.3%	23.8%	0.0%
05H	41.8%	51.9%	6.3%	0.0%
05P	36.5%	53.3%	10.2%	0.0%
05U	29.1%	54.0%	6.0%	10.9%
07AA	36.6%	56.9%	6.5%	0.0%
08C	36.8%	57.4%	5.8%	0.0%
10AJ	35.9%	48.0%	16.1%	0.0%
10AN	35.4%	57.2%	7.5%	0.0%
10AP	38.4%	48.5%	13.0%	0.0%
AM	33.9%	64.3%	1.8%	0.0%
Cr+Nb	32.5%	67.5%	0.0%	0.0%

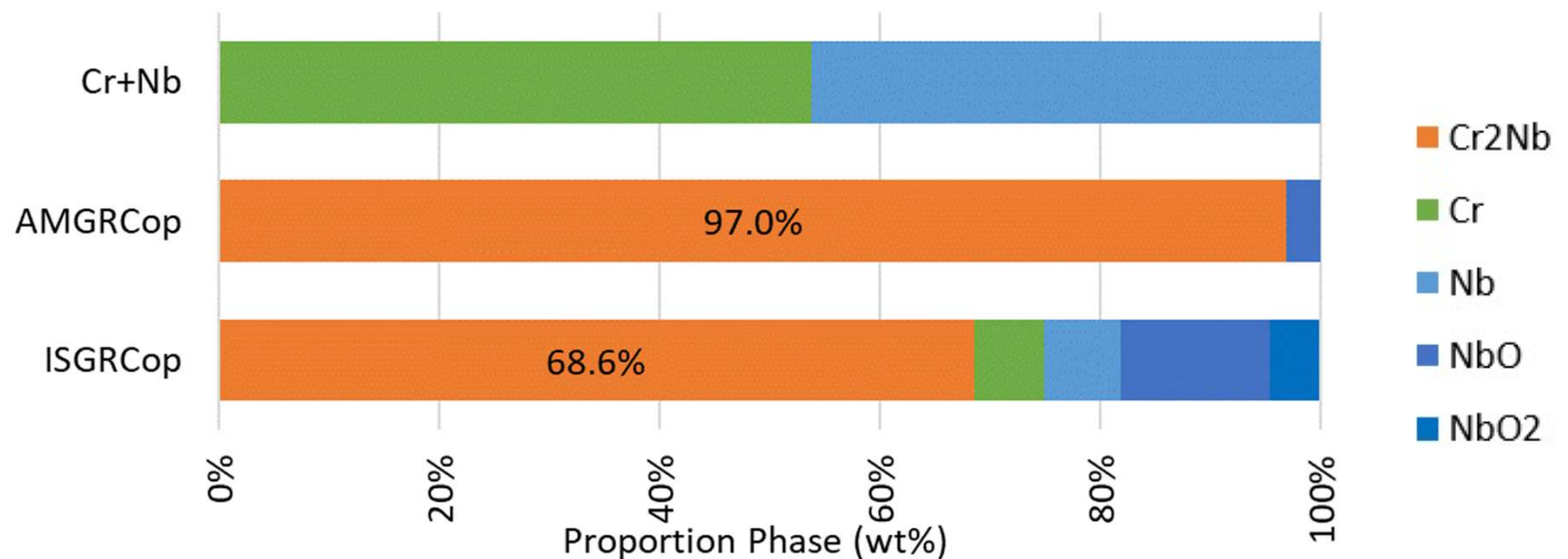
in situ versus Conventional AM

- AMGRCop, gas atomized GRCop powder which is used to printer AMed components of GRCop (AMGRCop: 97 wt% Cr_2Nb)
- This work: elemental powders used to print components and form GRCop in situ (10AN: 75.4 wt% Cr_2Nb , 10AP: 63.2 wt% Cr_2Nb)



Processing Impact on Extracted Dispersoid Phases

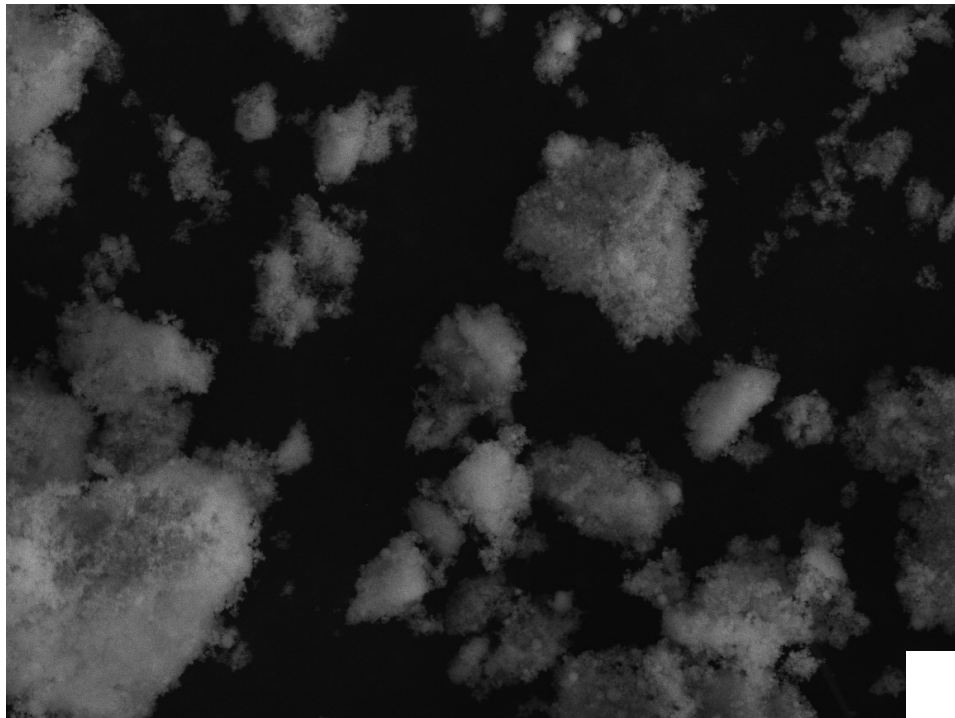
- ISGRCop remains well below reaction completion
 - Could be due to the hatch spacing issue, if the laser misses elemental powders they cannot react.
 - High O-content is in Nb-based oxides
- Oxides will continue to be monitored to identify their source.



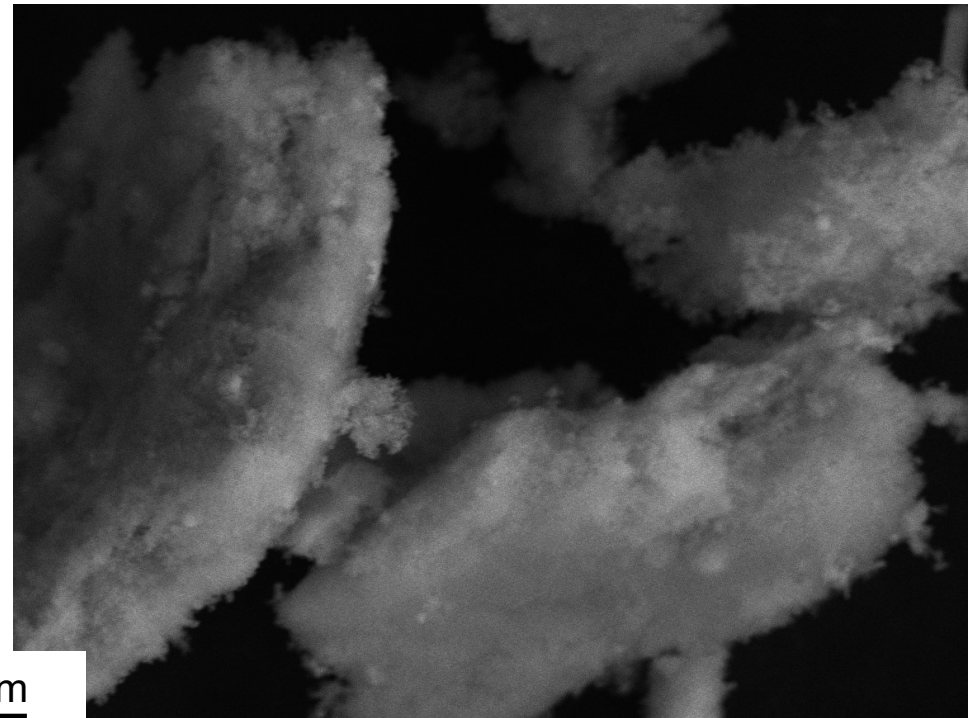
*AMGRCop contains two phases of Cr₂Nb

Precipitate Morphology

10AP (high O)



Conv. AM

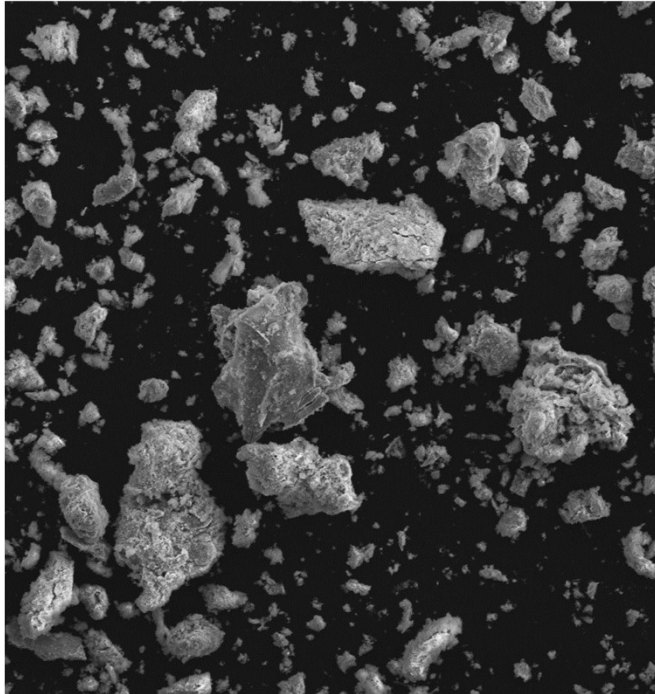


2 um

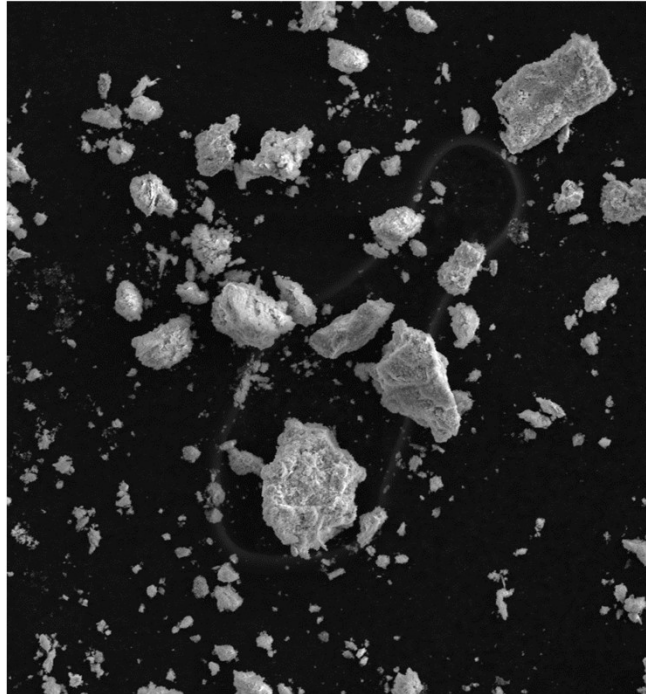
- Particles appear to have a foamy surface. Potentially due to
 - static charge attracting much smaller particles.
 - an AM-caused macrostructural effect.

Extracted Precipitate Morphology

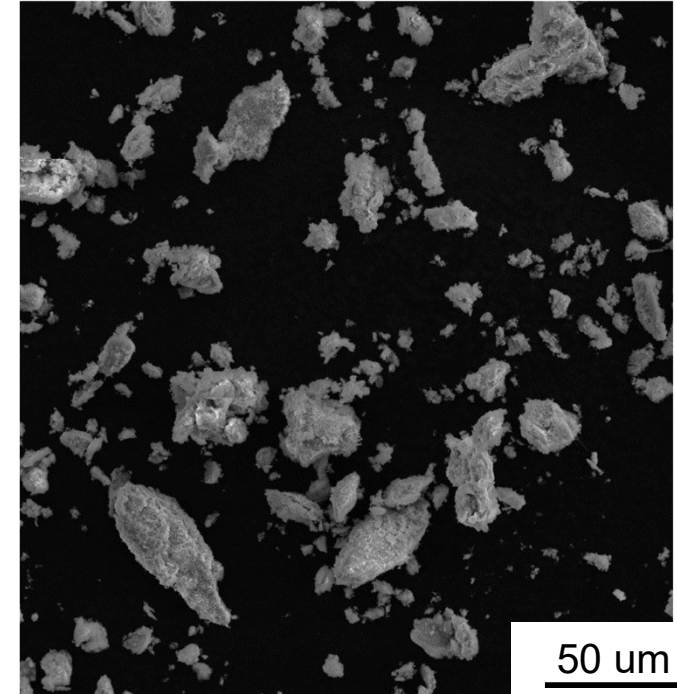
10AN (low O)



10AP (high O)

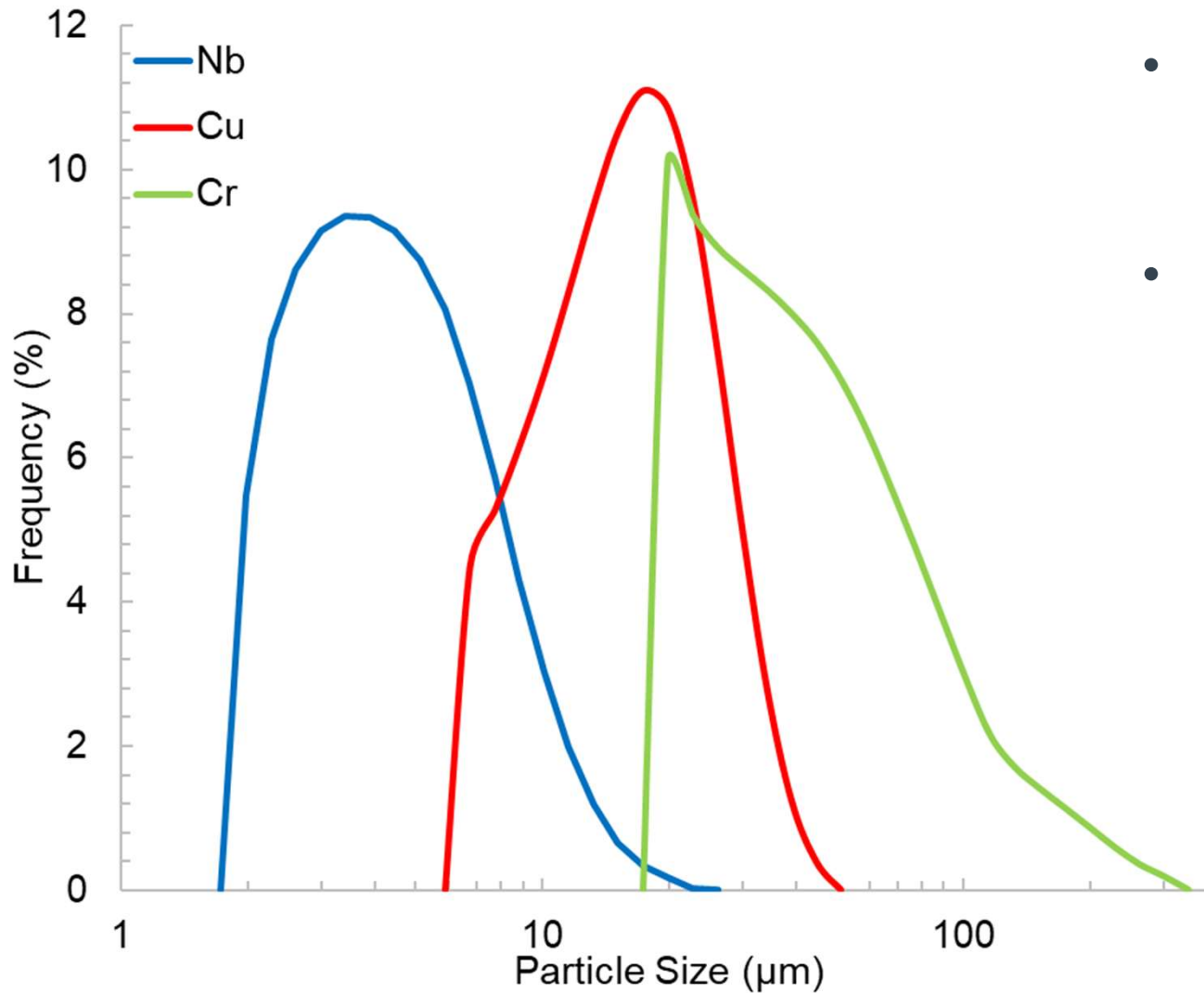


Conv. AM



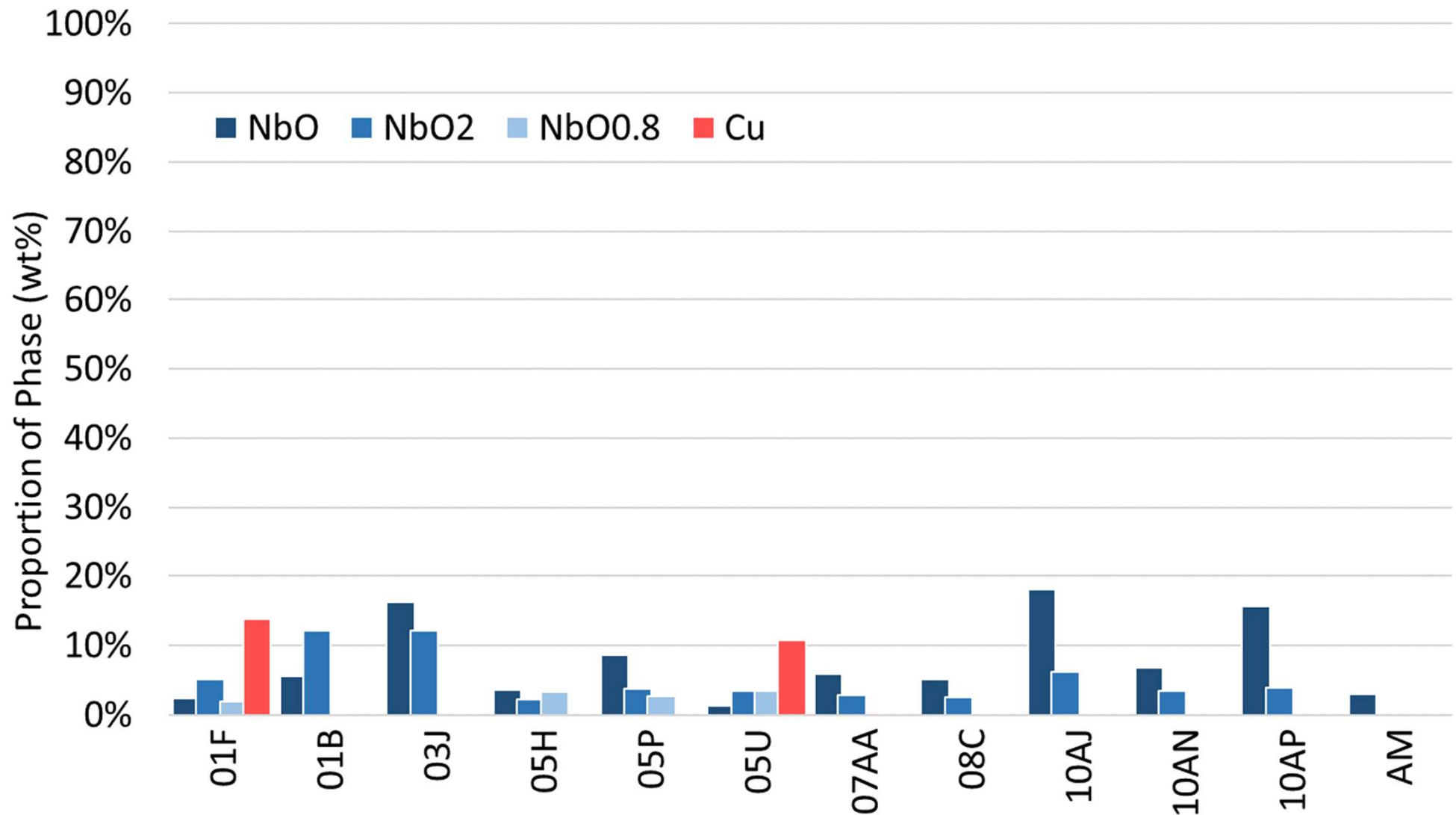
- Particle sizes and features are largely consistent across the differing chemistries and differing manufacturing procedures.

Powder Characteristics

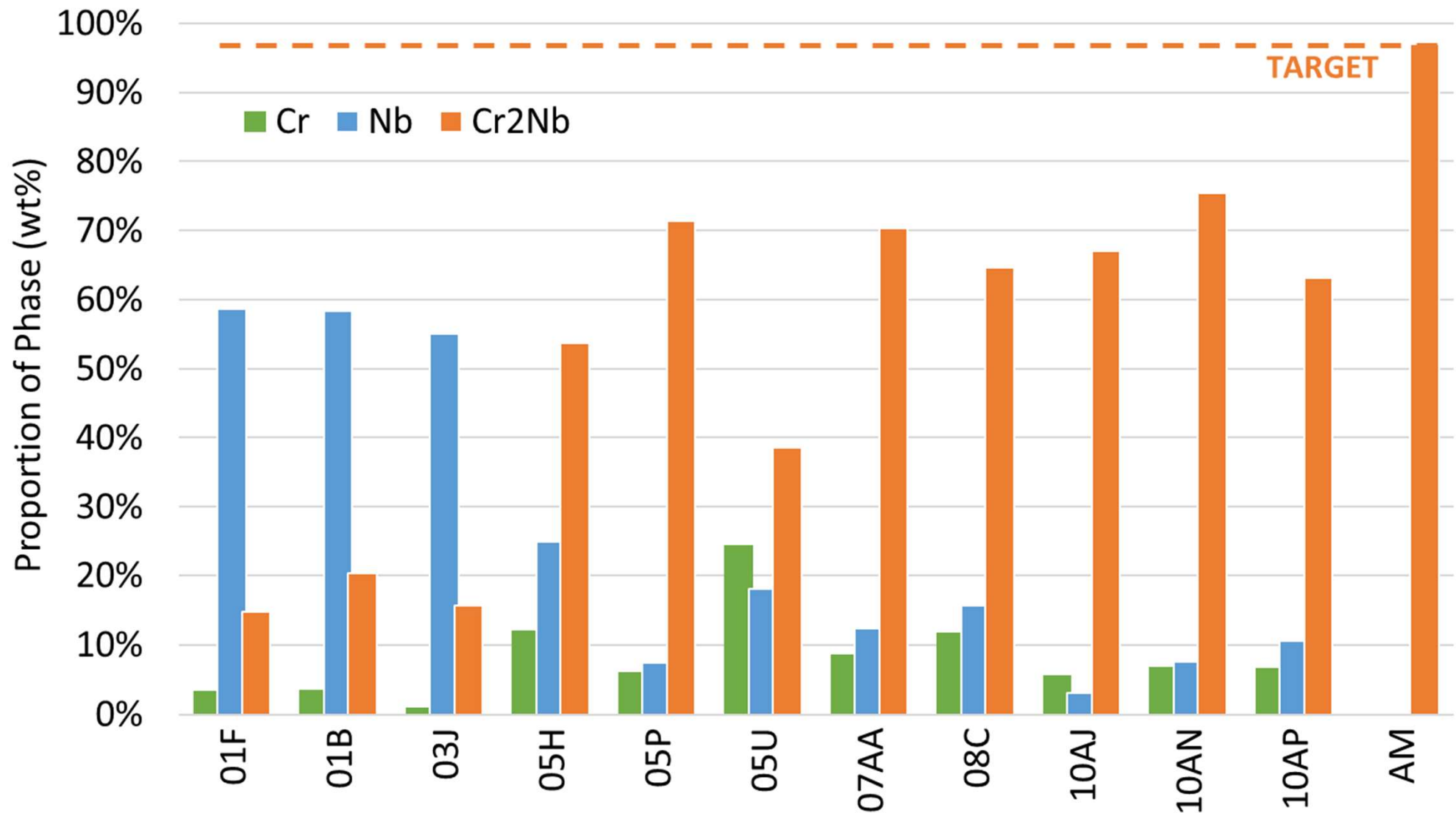


- First lots of Nb, Cu, and Cr shown, analyzed via Horiba Partica LA-960
- Seconds lots of Cr and Nb resemble the as shown Nb plot
 - Used for builds 6 - 10

Secondary Phases Identified



Primary Phases Identified

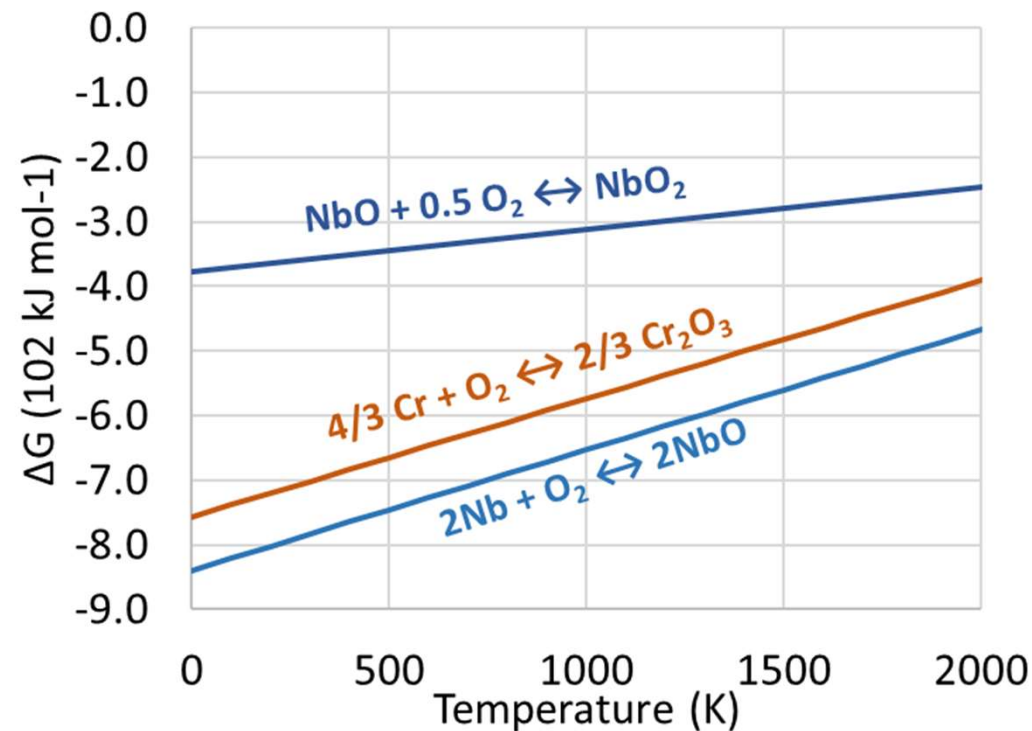


⁵ D. Scannapieco, et al. NASA/TM-20205003857, June 2020.

*AMGRCop has 2 Cr₂Nb phases

Secondary Phase Rational

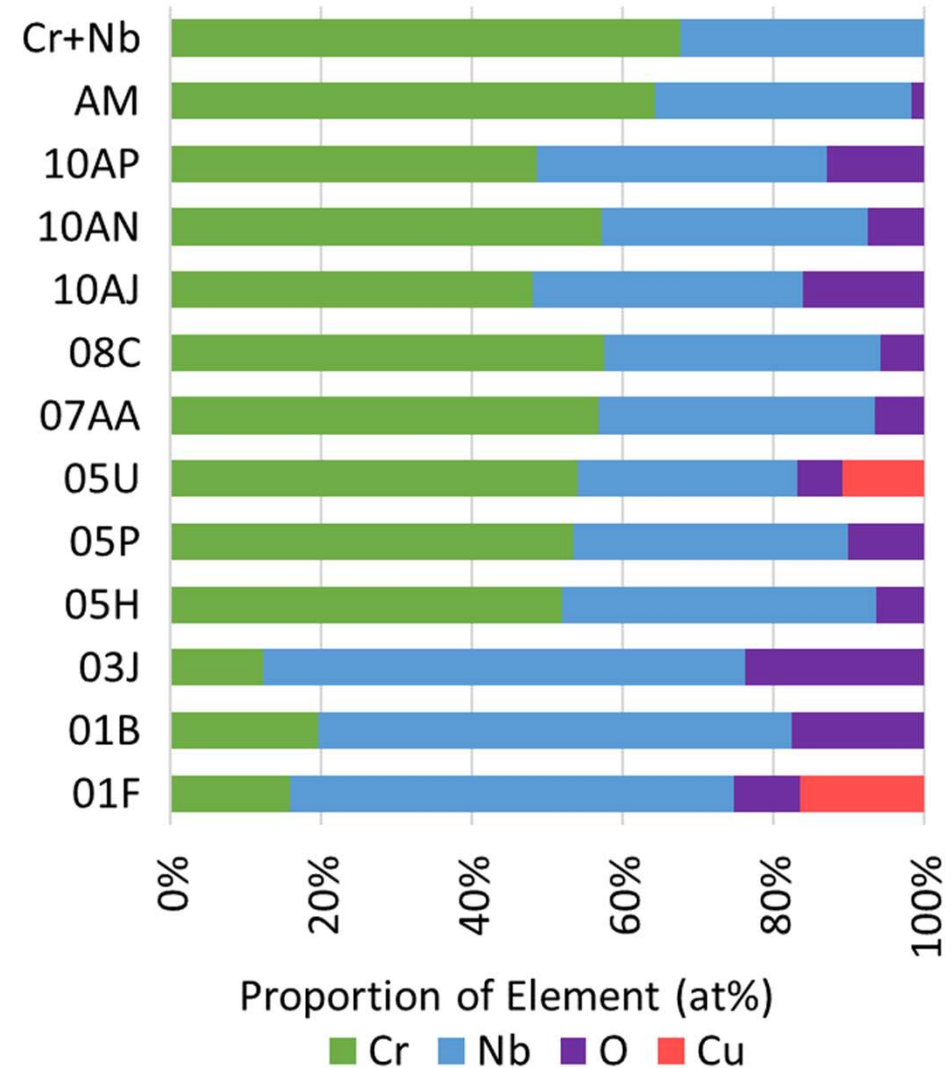
- Phase extraction not fully completed for 01F and 05U, presence of Cu
- Only Nb-based oxides present
 - Suggests that Cr-based oxides cannot survive laser processing
 - Or Cr-based oxides cannot survive nitric acid treatment
- NbO is most abundant oxide
 - Supported by free energy of formation
- No oxides present in milled Cr+Nb
 - Suggests formation in SLM
 - Or formation in nitric acid



⁵ Chase, M.W., Jr., J. Phys. Chem. Ref. Data, 1998, 1-1951.

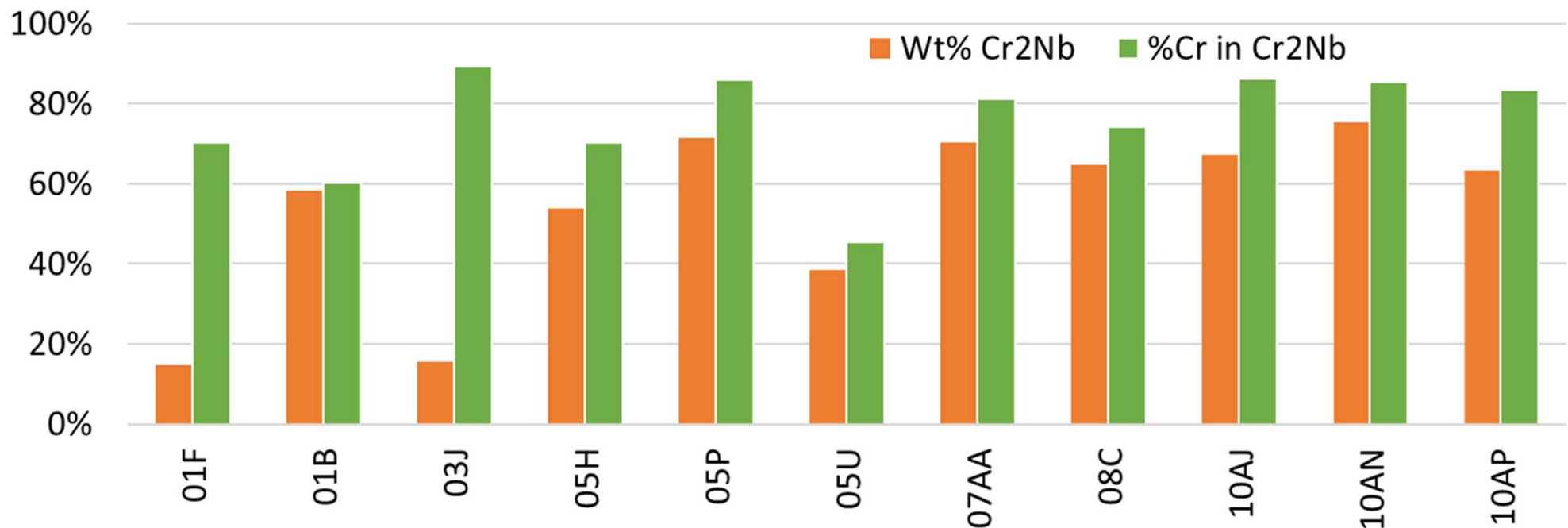
Cr Deficiency in Early Builds

- Builds 1 and 3 had insufficient Cr to fully form Cr_2Nb
 - Primarily due to large Cr powder size and sieving practices prior to printing
- Milled Cr+Nb and AM show target chemistry (66 at% Cr, 33 at% Nb)
 - Milled Cr+Nb used in builds 7, 8, and 10



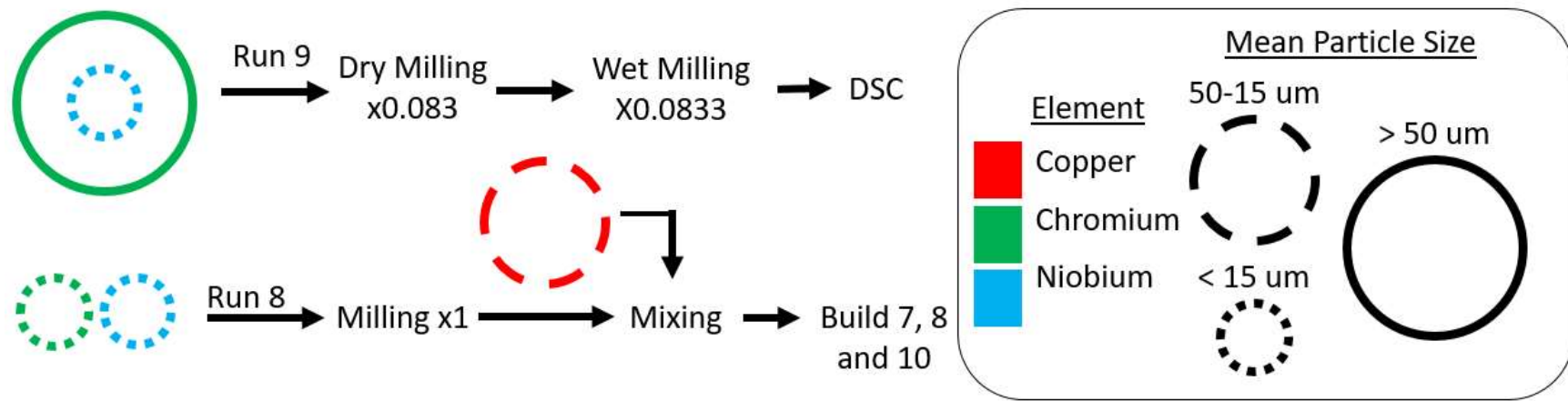
Parameter Analysis

- Due to Cr deficiency in early builds we convert wt% Cr₂Nb as the metric to proportion of Cr in Cr₂Nb
 - Cr is the limiting factor, new metric indicates proportion converted compared to what the potential Cr₂Nb amount was
- Biggest changes are for specimens with Cr deficiency

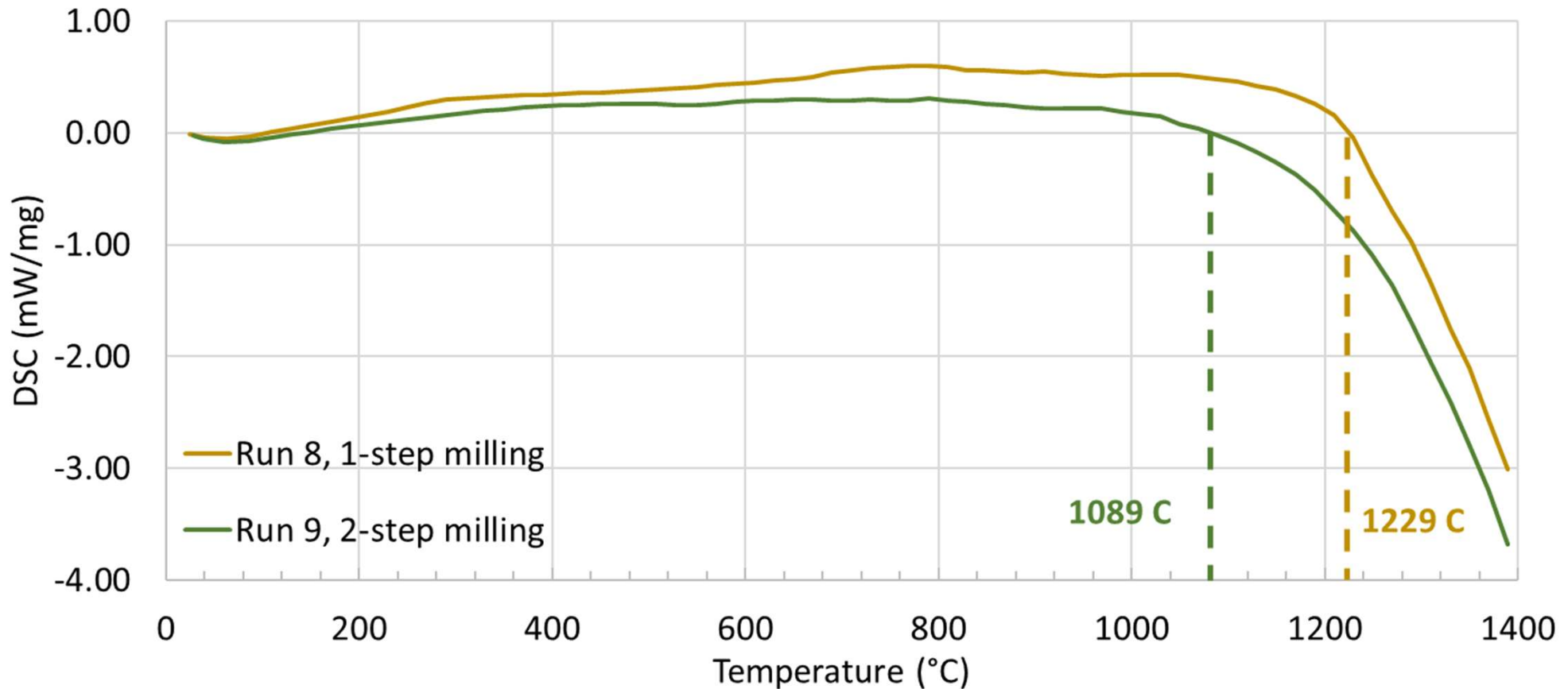


Differential Scanning Calorimetry

- Run 9 produced with Spex mill and 2-step milling procedure
- Goal was to produce smaller, more intimately mixed Cr+Nb powder
- DSC of Run 8 Cr + Nb, a 1-step milling procedure used as a comparison
- Run 8: 1-Step procedure (1-position planetary mill, HEBM):
 - 6.35 mm diameter bearings, dry milling at 10:1 BPR
- Run 9: 2-Step procedure (Spex Mill, HEBM):
 - 4.88 mm diameter bearings, dry milling at 10:1 BPR
 - 2.47 mm diameter bearings, wet milling at 10:1 BPR



Differential Scanning Calorimetry: Preliminary Results



- Transition to phase transformation 140 C lower temperature for Run 9 powder compared to Run 8
 - Some oxidation differences that need to be addressed

Differential Scanning Calorimetry: Preliminary Results

- Endothermic region of DSC confirmed to be due to Cr_2Nb phase transformation in Run 9 powders (2-step milling)
 - As with precipitates, powders are likely combination of Cr_2Nb , Cr, Nb, Cr-based, and Nb-based oxides after DSC
- Minute powder size differences between Run 8 and Run 9

